Effects of CO_2 on polymeric materials in the CO_2 transport chain: A review

Luca Ansaloni[a,*], Ben Alcock[b], Thijs A. Peters[a]

[a] *Thin Film and Membrane Technology Group, Department of Sustainable Energy Technology, SINTEF Industry, Oslo, Norway*
[b] *Polymer and Composite Materials Group, Department of Materials and Nanotechnology, SINTEF Industry, Oslo, Norway*

A B S T R A C T

The implementation of carbon capture and storage requires suitable solutions at all levels of the CO_2 value chain, including the CO_2 transport. A large number of studies in this area are dedicated to the characterization of metallic materials for pipelines, whereas limited data are available on the polymer-based materials needed for various components of the transport chain (such as gaskets, sealants, tanks, vessels, tubes, pipes). The present document aims to review the most recent information available in the open literature describing the influence of high density (dense phase) CO_2 on elastomers and engineering thermoplastics suitable for operations within the CO_2 transport process. First the operative ranges for both ship and pipelines transport are identified, and the most important physical properties and involved phenomena are described. Subsequently, the effects of highly concentrated CO_2 phases on selected polymer families are analyzed and, finally, the influence of impurities in the CO_2 stream is summarized. This works highlights the presence of large gaps of knowledge base which leave open questions and challenges to be solved by the CCS community to ensure that the full-scale deployment becomes a reality.

1. Introduction

Carbon capture and storage (CCS) is accepted by the international scientific community as the most viable short-term measure to limit CO_2 emission in the atmosphere, avoiding reversible changes on the planet's climate. The International Energy Agency (IEA) states in Energy Technology Perspectives (ETP) 2017 that in order to limit the global temperature increase to 2 °C, energy and process-related CO_2 emissions should be reduced by almost 60 % by 2050 compared to 2017 levels (International Energy Agency, I., 2017). When excluding emission reductions from efficiency improvements, the expected contribution of CCS to this decrease is 30 %. The achievement of a full-scale CCS deployment relies on efficient and reliable solutions at all levels of the value chain (Størset et al., 2018). Whereas capture and storage are steps of primary importance to allow a reduction of the carbon emission, viable and economically feasible CO_2 transport solutions must be ensured to enable the CCS deployment. In particular, avoidance of leakages or failures within the entire transport chain is key to ensure the viability of the process, assuring that the efforts of CO_2 capture are not diminished during transportation.

Fig. 1 shows a schematic version of the CO_2 value chain within the CCS scheme, which is composed of 3 main steps: capture, transport and storage (Gassnova and Gassco, 2016). Sequestration of CO_2 from the emission sites can be carried out by means of different technologies (i.e., adsorption, absorption and membrane technologies) depending on the capture process involved. Subsequently, the CO_2 is transported to the storage location, where it is injected and permanently sealed through impermeable rock formations in deep saltwater reservoirs or depleted oil/gas fields. In view of the public perception on storage options (onshore compared to offshore), offshore reservoirs offer a more feasible solution on the short term compared to onshore sites for permanent CO_2 storage (Haug and Stigson, 2016; Margriet Kuijper, 2011). Emission points can therefore be expected to be located far from the injection wells, requiring an efficient infrastructure for temporary storage and transport of CO_2. Pipelines and ships (Kjärstad et al., 2016; Roussanaly et al., 2013) represent the most viable solution to transfer the captured carbon dioxide between the emission source and the storage site, and the choice of transportation mode depends on the emission capacity and the distance to be covered. Multimodal transport systems are suggested to minimize the transport costs (Geske et al., 2015a, b), with pipelines preferred for short distances and large emission capacity, whereas ships are more effective in the case of long distance and lower emission capacity. In the early stage of CCS deployment, the higher flexibility of ships and vessels is expected to offer a more suitable short-term solution for areas with no existing pipelines infrastructure (Kjärstad et al., 2016). This is for example the case for

---

* Corresponding author.
E-mail address: luca.ansaloni@sintef.no (L. Ansaloni).

Nomenclature		NO$_x$	Nitric oxides
		PA	Polyamide
ABS	Acrylonitrile butadiene styrene	PC	Polycarbonate
CCS	Carbon capture and storage	PEEK	Polyetheretherketone
CR	Chloroprene rubber	PES	Polyether sulfone
CSM	Chlorosulfonated polyethylene rubber	PET	Polyethylene terephthalate
EPDM	Ethylene propylene diene monomer rubber	PP	Polypropylene
EVM	Ethylene vinyl acetate rubber	PTFE	Polytetrafluoroethylene
FKM	Perfluoro rubber	PVDF	Polyvinylidene difluoride
FEPM	Tetrafluoro ethylene/propylene rubbers	PVC	Polyvinyl chloride
H$_2$S	Hydrogen sulfide	RGD	Rapid gas decompression
HDPE	High density polyethelene	SBR	Styrene butadiene rubber
HNBR	Hydrogenated nitrile butadiene rubber	SO$_x$	Sulfur oxides
IR	Isoprene rubber	Tg	Glass transition temperature
NBR	Nitrile butadiene rubber		
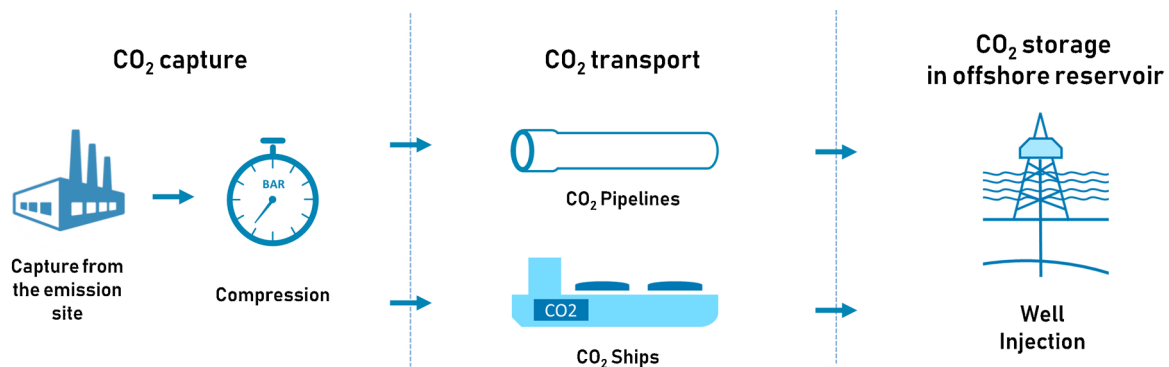
Fig. 1. Representation of the CO$_2$ value chain.

Europe where, unlike in the US where a large CO$_2$ pipeline infrastructure has been established for EOR (Enhanced Oil Recovery) purposes, the existing pipeline grid is limited (Global CCS Institute, G., 2017; Noothout et al., 2014). Of course, the use of existing infrastructure in CO$_2$ transport should be assessed to ensure that the materials used would also be suitable for the specific conditions in CCS applications (Parker et al., 2009). In addition, the flexibility of ships and vessels may play an important role in collecting the CO$_2$ from sites with intermittent emissions, requiring also feasible solutions for temporary storage.

Regardless of transportation mode, to increase the transport efficiency, CO$_2$ needs to be transported as liquid or supercritical fluid (i.e., high storage density). Although considerable attention has been paid to metallic CO$_2$ pipelines, both in terms of design (DNVGL, 2017; Johnsen et al., 2011; Patchigolla and Oakey, 2013; Zhao et al., 2016) and effects of contaminants (Dugstad et al., 2013; Halseid et al., 2014; Seevam

et al., 2008; Skaugen et al., 2016; Wetenhall et al., 2014b), a lot of uncertainty surrounds the effect of CO$_2$ on polymeric materials such as elastomers and engineering plastics. As showed in Fig. 2, when pipelines are used, a limited number of steps are involved in the transport process: compression, transfer through an onshore pipeline, pumping and transfer through an offshore pipeline to a platform can be summarized as the main steps. Nevertheless, when the transportation is by ship, several steps are involved (Geske et al., 2015a). In view of the intermittent nature of the ship-mode transport, high-density storage solutions (i.e. liquefaction) will be favored and temporary storage options must be implemented to allow a buffer between each loading and unloading operation. Before the final transfer to the permanent storage site, the liquid CO$_2$ needs to be heated and pumped to achieve the standard operating conditions for injection into the well. Therefore, all the non-metallic components used in tubes, piping, tanks, compressors, pumps and other components of the value chain can be exposed to
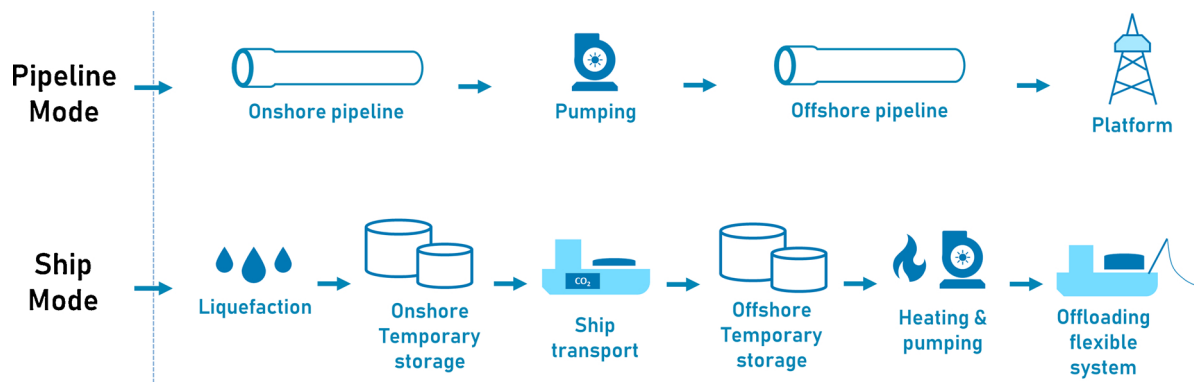
Fig. 2. Steps involved in the CO$_2$ transport process via pipelines or ships.

conditions that are outside the typical operating range for these materials, increasing the possibility of failure and unwanted emissions.

The transport of dense or liquid CO_2 represents a challenge for all the materials which come in contact with it. Metal components are typically the materials of choice for pipes, containers and valves due to their combination of high mechanical properties, relatively low cost and established history of use. However, many metals are susceptible to increased corrosion in contact with CO_2 (Xu et al., 2018), which can accelerate material failure and therefore reduce the service life of the parts (DNVGL, 2017). On the other hand, polymeric materials can be used as barriers to protect metallic components from CO_2, in addition to their use as seals between mating metal components to prevent leakage. However, polymeric materials can also be affected by the local physical and chemical environment and may undergo temporary or permanent changes in structure that can in turn affect their performance. The relationship between exposure to dense or liquid phase CO_2 and changes in material performance are complex and not widely reported. To start to address this, the present work aims to summarize the latest findings on the effect of CO_2 on non-metallic materials that can be used within the CO_2 transport chain, in industrially relevant conditions. Transport in pipelines involves CO_2 compressed at 10–20 MPa (above the critical pressure of 7.5 MPa, to avoid multiphase flow) at ambient temperature. Under these conditions, various polymeric materials may undergo changes in mechanical properties due to physical and chemical interactions with CO_2, especially when CO_2 is in the supercritical state. Optimization of ship transport efficiency is reported to require cryo-compressed conditions, that can vary between 15–20 bar at −30 °C to triple point conditions (Equinor et al., 2018). This last condition may be critical for a wide range of polymer materials, as the temperature may decrease to, or already be below, the glass transition temperature of the majority of plastics available on the market. In addition, continuous loading and unloading cycles (i.e., rapid gas decompression cycles) under cryo-compressed conditions may have an unpredictable impact on the physical properties of these materials.

2. Fundamental aspects

2.1. Operating conditions for CO_2 pipelines and ships

Carbon dioxide (CO_2) is a naturally occurring, colourless gas currently accounting for approximately 410 ppm of atmospheric gas and has a density of 1.98 kg·m^{-3} at STP. Pure CO_2 has a phase diagram as shown in Fig. 3. Above −50 °C (223 K), the CO_2 is expected to be liquid or gas if the pressure is < 400 bar (40 MPa). Cost-effective transport requires a high density of the fluid to be transported and for this reason CO_2 is often transported as a liquid or a supercritical fluid. Accordingly, Fig. 3 shows the operation envelopes for transport by pipelines and by ship. In the case of pipelines, the operating temperature is fixed by environmental factors (pipelines are exposed to atmospheric conditions). CO_2 is often transported at pressure greater than the critical pressure (7.4 MPa), to avoid multi-phase flow. It is inherently more efficient to transport a liquid than a gas, and the supercritical fluid is typically over-pressurized to ca. 10 MPa to compensate for pressure losses to maintain the supercritical state (Santos, 2012). Transport of CO_2 by ship has existed already for 30 years, related to industrial or alimentary purposes, with the operating ranges being around 15–20 bar and −30 °C. Nevertheless, due to the large volumes of CO_2 to be transported in the CCS process, conditions closer to the triple points (7–9 bar and −55 °C) are needed to increase the fluid density and reduce the overall transport costs (Zero Emission Platform, 2011). Data on the pressure-volume-temperature (PVT) relationship of CO_2 at sub ambient temperatures have also been reported elsewhere in literature to 233 K (Aspelund et al., 2006; Brachthäuser et al., 1993; Klimeck et al., 2001).

The phase diagram shown in Fig. 3 is for pure CO_2. However, the presence of impurities in the CO_2 stream can alter the phase diagram depending on the concentration (Aursand et al., 2016). For example,

models of the effect of 0.01 mol% (100 ppm) – 20 mol% of nitrogen on the phase behaviour of CO_2 have been reported, to predict the shift in the critical point (Goos et al., 2011). It is also important to note that, when small amounts (2 mol%) of impurities (H_2S, NO_2, or H_2S) are present in the CO_2 stream, a dual phase region will be created above or below what would be expected for the pure CO_2, depending on the critical temperature (T_c) of the impurity (Wetenhall et al., 2014b). In particular, if the critical temperature of the impurities is above that of CO_2 (e.g., H_2S and NO_2), the 2-phase region will be found below the critical temperature of the pure CO_2 and vice versa (Wetenhall et al., 2014b). Formation of a 2-phase region during the CO_2 transportation in pipelines has been reported to have tremendous impact on the pressure drop (Verma et al., 2011). A detailed analysis of the impurities' effect on the physical properties of CO_2 mixtures has been reported by Seevam et al. (2008).

The critical pressure of the mixture containing impurities increases independently from the critical temperature of the impurities present, determining an increase of the operative pressure required to avoid 2-phase flow (Knoope et al., 2013). At the same time, the presence of components with a critical temperature (T_c) below that of CO_2 will lower the critical temperature of the mixture, whereas the opposite trend is expected for the ones with a higher T_c (Wetenhall et al., 2014b). Finally, minor components are also reported to significantly affect the economic feasibility of liquified CO_2 transport by ship. In the scenarios considered (various impurities with concentration down to 0.5 mol%), the higher pressure required made the process economically unfeasible and the authors suggested further reductions of impurities' level to reduce the influence (Wetenhall et al., 2014a). A peculiar behaviour is also observed in presence of water. In the case of dense CO_2, the water content can lead to different states of water molecules: if the water content is below the solubility limit, the water simply dissolves in the CO_2, but if the water amount exceeds the solubility limit, the water molecules will tend to condense, attracting CO_2 and impurity molecules (e.g. SO_x, NO_x, H_2S, and O_2) (Xiang et al., 2017). Furthermore, this solubility limit is dependent on the amount of other impurities present in the CO_2 mixture (Munkejord et al., 2010). In the case of dense phase CO_2, the water solubility is found to increase with the operating temperature and pressure (King et al., 1992). Morland et al. (2017) showed that above 20 °C, the water content in dense phase CO_2 (pressure 100 bar) can reach 3000 ppmv, but when the temperature is decreased below −5 °C this value is already halved.

2.2. Effect of CO_2 on polymers

The high CO_2 density requirements described in the previous paragraphs pose a major challenge for the stability of polymeric
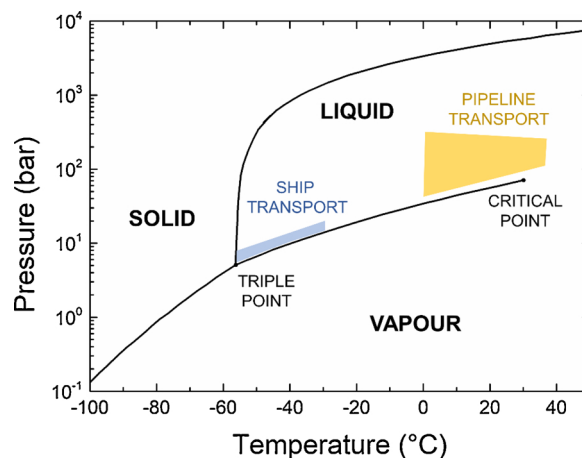

Fig. 3. CO_2 phase diagram. Approximate operative ranges for transport in pipeline and ship-mode have been sourced from (Knoope et al., 2015).

materials, and the most important ways in which CO_2 can affect different polymers will be summarised here. Liquid phase CO_2 has the potential to be a good solvent for many elastomers and engineering thermoplastics (Global CCS Institute, 2010) and this effect is also mentioned in the DNVGL Recommended Practice document: "Design and operation of carbon dioxide pipelines" (DNVGL, 2017). CO_2 is widely used in combination with polymers as a reaction solvent, foaming agent (Davies et al., 2008; Wang et al., 2012), or to transport chemicals into (Belhadj-Ahmed et al., 2009) or out of materials, such as residual solvents (Davies et al., 2008; Srisang et al., 2014) (especially for supercritical CO_2). CO_2 is reported to be a good solvent for non-polar and some polar low molecular weight polymers, but a poor solvent for some high molecular weight polymers (below 100 °C and 350 bar) (Kendall et al., 1999). The Hansen solubility parameters offer the opportunity to account for interactions between polymers and solvents, as they are based on the description of the cohesive energy of molecules by means of 3 different contributions: Van der Waals forces, polarity and hydrogen bonding (Hansen, 2004; Williams et al., 2004). Differences in solubility parameter below 2 digits are expected to lead to significant absorption of the solvent into the polymer phase. This may result in significant swelling of chemically crosslinked polymers (such as most elastomers) or can even lead to complete dissolution of polymers which are not chemically crosslinked (e.g. thermoplastic polymers). Fig. 4 compares the solubility parameters of liquid CO_2 with the solubility parameters of typical elastomers and thermoplastic materials, showing qualitatively their affinity with CO_2. Clearly, the parameter ranges are quite similar in case of many elastomers and, even though the chemical crosslinking present in these elastomers prevents their dissolution in liquid CO_2, high uptake (and therefore large volumetric swelling) may be expected. Different values are observed in the case of the thermoplastics, such as high-density polyethylene (HDPE) or poly-tetrafluoroethylene (PTFE), which would therefore be expected to be more stable in presence of liquid phase CO_2.

Some simple polymers have even been designed to act as sponges to absorb CO_2 from a mixed gas feed either in the intermolecular free volume (Woodward et al., 2014) or in pores in the microstructure (Huang et al., 2017; Mane et al., 2017; Wang et al., 2017). Other polymer families, such as siloxanes (silicone elastomers) and some fluoropolymers show unusually high CO_2 sorption at lower temperatures and pressures (Davies et al., 2008), whereas some fluoropolymers can be dissolved at higher temperatures and pressures (Tuminello et al., 1995). In siloxanes, this is probably due to interactions with the ether linkage (-R-O-R'-) (Zhao et al., 1995), while in fluorinated polymers, this may be due to the interaction between CO_2 and the C–F bond (Davies et al., 2008).

Large CO_2 uptake within the polymer matrix may lead to plasticization phenomena, which can be defined by changes in mechanical performance, a shift in Tg or an increase in CO_2 permeability (Bos et al., 1999). Specifically, CO_2 absorption can lead to a reduction in stiffness (resistance to elastic deformation) and an increase in toughness (resistance to crack propagation). This decrease in stiffness observed in a material after the absorption of CO_2 may occur by a combination of two mechanisms. Firstly, absorbed CO_2 may act on the molecular level as a lubricant (or plasticizer), reducing molecular interactions between polymer chain and allowing the molecules to move past each other more easily. This allows easier deformation on the macroscale (and so a reduction in stiffness). Secondly, the accumulation of CO_2 can swell the volume of the structure (Daou et al., 2014), meaning that less polymer is present per macroscopic unit volume. Therefore, as there is less polymer material per unit volume to resist deformation, the structure is inherently less stiff and also more permeable to gases or liquids. An increase in volume can also lead to geometrical mismatches, seal extrusions, part warpage and other engineering problems. Polymers with polar and flexible pendant groups (such as $-COOCH_3$ or $-OCOCH_3$) are reported to be especially susceptible to plasticization by CO_2 (Bos et al., 1999; Puleo et al., 1989). Sawan et al. report the changes in

mechanical properties and plasticization for a range of polymers after exposure to CO_2 at various pressures (Sawan et al., 1994).

Supercritical (or dense phase) CO_2 is reported to have a high solvation capability, and for this reason is used to increase the purity by extracting impurities from polymeric materials used in medical and pharmaceutical applications (Barnes, 2001; DeCrosta and Jagnandan, 1999). This "extraction ability" can also lead to the undesired removal of plasticizers or other non-bonded additives out of polymers, resulting in significant changes of their chemical and physical properties. Plasticizers are chemical additives which are often not chemically bonded to the polymer chains but can instead reside in the free volume between the polymer molecules. Although it has been described above that CO_2 itself may plasticize polymers, CO_2 may also have a de-plasticizing effect. The loss of plasticizer chemicals from the intermolecular free volume of the material due to an exchange with CO_2 may lead to an increase in stiffness after CO_2 exposure. The extraction of plasticizers (or other non-chemically bonded additives) may also result in a volumetric shrinkage (Paul et al., 2012). In a sealing application, volumetric shrinkage could lead to seal leakage, as well as local mechanical stresses, potentially causing warpage, debonding or cracking. Examples of other additives present in many polymers are anti-oxidants, UV-stabilizers, flame retardants or pigments (Global CCS Institute, 2010). The severity of any additive removal effect would be dependent on the amount of additive present in the polymer matrix, how easy they can be removed and how critical they are to the function of the material.

The degree of CO_2 absorption is also affected by morphology (structural order) of the polymers. Polymers are either entirely amorphous (lacking regular structure) or semi-crystalline (comprising local regions of dense crystals and amorphous regions). Generally amorphous polymers have more free volume than the crystalline regions of semi-crystalline polymers, and so the presence of crystallinity would be expected to hinder CO_2 mobility (Doroudiani et al., 1996; Michaels and Bixler, 1961; Shieh et al., 1996b). However, the swelling on the amorphous regions may also lead to some loss of crystallinity (Takajo et al., 2008), so a complex relationship between CO_2 absorption and crystallinity in polymers can be expected for semi-crystalline polymers, such as HDPE or PP.

A key factor which determines which polymers can be used in different applications is the glass transition temperature (T_g). Above this transition temperature, the molecules in amorphous polymers (or of the amorphous phase of semi-crystalline polymers) have enough thermal (vibrational) energy to have a larger degree of freedom of movement. When heating a polymer through this glass transition region, the increase in molecular movement is usually detectable by a decrease in mechanical stiffness and an increase in toughness and deformability. In
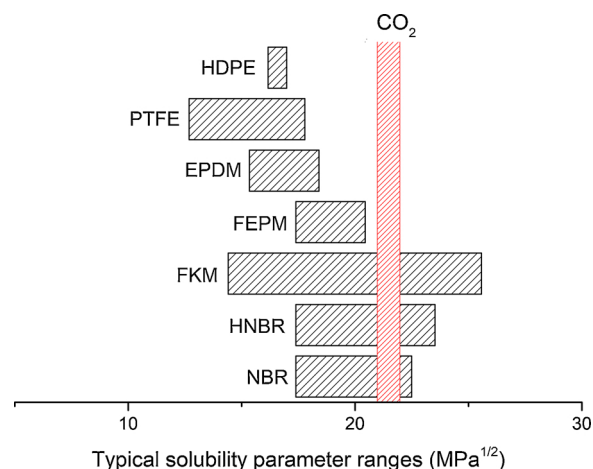

Fig. 4. Solubility parameters for liquid CO_2 and some polymers at room temperature (data from (Global CCS Institute, 2010), (Ebnesajjad, 2015), (Zhang et al., 2010)). Temperature is expected to significantly affect these parameters.

contrast, below the T_g, polymers are typically hard and brittle. Polymers used in sealing applications (mainly elastomers) are usually operated above T_g since in the glassy state elastomers can be too stiff to maintain good contact during thermal contractions of mating components, increasing the leakage around the seals (Akulichev et al., 2018). Due to thermal contraction, there is also an increase in density of polymers during cooling, and this increase in density hinders CO_2 diffusion. Similarly, the swelling in CO_2 would result in a decrease of density and also a downwards temperature shift in T_g of that polymer (Alessi et al., 2003; Kazarian, 2000). To visualise this effect, a decrease in T_g of a polymer would mean that a polymer may be less stiff and more tough than would normally be expected of that polymer at a given temperature. For example, a decrease of several tens of degrees in T_g has been reported in PES (polyether sulfone – a semi-crystalline polymer) after the CO_2 pressure was increased from 7.8 to 35 bar at 100 °C (Bos et al., 1999; Sanders, 1988). In addition to effects such as changes in stiffness, increased molecular mobility due to CO_2 absorption would also be expected to change long term performance such as a reduction in creep resistance (increased deformation under permanent loading, or seal extrusion).

It should be noted that although T_g is usually specified as a single temperature point, it would be more correct to consider the T_g to be a temperature range. This is because polymer materials always have some variation in properties such as molecular weight and molecular imperfections which influence the T_g. The broadness of the T_g temperature range is important when considering the application of polymers which have a T_g just below the lowest expected application temperature. For example, if EPDM (an elastomer based on ethylene propylene diene monomers) with a $T_g = 54$ °C was used at −50 °C, some stiffening of the polymer may already occur, even though the application is slightly above the specified T_g.

2.3. Rapid gas decompression (RGD) damage

Rapid gas decompression (RGD) damage is typically reported as a major issue for polymer-based materials when operated at high pressures and then subject to one or more depressurization events, due to the high large gas sorption in the polymers (Briscoe et al., 1994). RGD damage is caused by gases which have been absorbed into a polymer under high pressure quickly expanding when the external environment is rapidly depressurized. If the expanding gas cannot diffuse out of the polymer fast enough, local expansion of the gas leads to supersaturation, bubble nucleation, bubble expansion and blistering or tearing of the polymer (Davies et al., 1999; Paul et al., 2012). Therefore, RGD damage can occur after a single depressurization event, although cumulative fatigue processes due to several less severe decompression events could also occur. Since elastomers typically have a high free volume, they are especially sensitive to RGD damage compared to other polymers. RGD damage testing is standardised in ISO 23936-2 (based on Norsok M710), with a typical decompression rate at 20 bar/min. Other standards, such as ISO 13628-2 are reported to use higher decompression rates (70 bar/min) (Wang et al., 2013), whereas some studies report changes in material properties after decompression rates of 0.3 or 5 bar/min (Abas et al., 2014). Since some degree of porosity may be expected in most elastomers as manufacturing defects (Ho, 2006), these are potential starting points for gas accumulation under pressure, and subsequent expansion when the external pressure is removed. RGD damage is typically a concern for elastomeric materials, although any material which has the potential to absorb CO_2 may also be susceptible to RGD damage if rapidly depressurized after saturation.

The sensitivity to RGD damage is determined by a number of factors (Paul et al., 2012; Schrittesser et al., 2016) including:

- the diffusion rate of the gas through the polymer (the faster the gas can leave the polymer, the lower the local pressure build up);
- the partial pressure of the soluble gases in contact with the polymer;
- the rate of RGD (the faster the depressurization, the less time the gas has to diffuse out of the polymer);
- the solubility of the gas in the polymer (the lower the amount of absorbed gas, the lower the local expansion on depressurization);
- the mechanical properties of the polymer (the tougher the polymer is, the less likely that local deformations will lead to crack propagation, while the stiffer the polymer is, the more local gas expansion is required to cause deformation);
- the depressurization temperature (virtually all properties of polymers are temperature dependant, so the RGD temperature affects the previous factors. For example, the toughness of a polymer is dramatically lower if tested below T_g, and therefore RGD damage

Table 1

Non-exhaustive list of polymers that may be found in the CO_2 transport chain, with their typical glass transition temperatures (Abas et al., 2014; Energy Institute London, 2010; Fergestad and Løtveit, 2014; Hertz, 2012; Tebodin Netherlands, 2011).

Polymer	Acronym	Tg (ºC)	Type of component
Elastomers			
Ethylene-propylene diene monomer	EPDM	−54	Sealants, gaskets
Chlorosulfonated polyethylene rubber	CSM	−55	Sealants, gaskets
Fluoroelastomers	FKM, FFKM, FEPM	−15 to 3	Sealants, gaskets
Nitrile butadiene rubber	NBR	−38 to −2[3]	Sealants, gaskets
Styrene butadiene rubber	SBR	−65 to −50[4]	Sealants, gaskets
Ethylene vinyl acetate rubber	EVM	−25 to 0[5]	Sealants, gaskets
Chloroprene rubber	CR	−45	Sealants, gaskets
Isoprene rubber	IR	−70	Sealants, gaskets
Engineering Thermoplastics			
Polypropylene	PP	−20 to 0[1]	Tubes, pipes
High density Polyethylene (usually PE100)	HDPE	−135 to −115	Tubes, pipes, tanks, vessels
Polyamides (Nylon, such as PA11 or PA12)	PA	40 to 60	Tubes, pipes, tanks, vessels
Polytetrafluoroethylene	PTFE	See note [2]	Tubes, pipes, sealants, gaskets
Polyvinylidene difluoride	PVDF	−35	Tubes, pipes, sealants, gaskets
Polyetheretherketone	PEEK	145	Higher temperature valves

[1] depending on the tacticity;
[2] the T_g of PTFE is subject to scientific debate (Calleja et al., 2013); however, PTFE is typically tough even at low temperatures.
[3] depending on the acrylonitrile content;
[4] depending on the production process (polymerization in solution or emulsion);
[5] depending on the copolymer composition (amount of ethylene vs vinyl acetate).
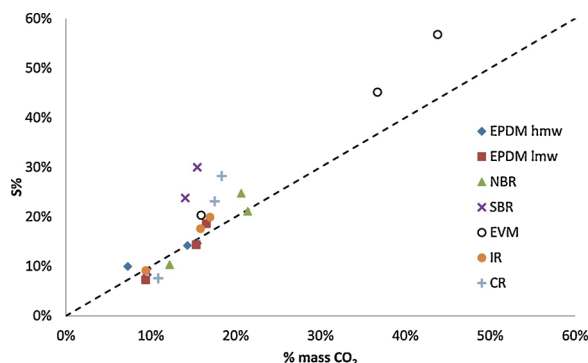
Fig. 5. Relationship between CO_2 sorption and swelling in different elastomers (T = 50 °C). Reprinted from (Dubois et al., 2018) with permission from Elsevier. The 3 different datapoints reported for each series refer to measurements performed at 5, 10 and 15 MPa.

would be expected to be very much greater if RGD were to occur below the T_g of the polymer).

A non-negligible aspect of RGD is related to the temperature drop that is expected due to the rapid gas expansion. Since the heat required from a phase transition in rapidly expanding CO_2 cannot be harvested from the environment, it has to be supplied by the fluid itself (Eldevik et al., 2009; Ho, 2006; Richardson and Saville, 1991). The temperature drop is a function of the depressurization range and the fluid type. The investigation of the blowdown of a CO_2 pipeline showed that the temperature drop is dependent on the decompression rate: for small decompression rates the associated ΔT is limited to few degrees, but in case of sudden rapture the fluid can get close to the triple point conditions (Guo et al., 2017, 2016).

3. Polymeric materials relevant to use in the CO_2 transport chain

In the CCS value chain, polymeric materials can be found in different components. Typically, they can represent the constructional material of pipelines, tanks, sealants and gaskets. In the case of pipelines and tanks, polymer materials may be preferred to metals due to the much lower density (i.e. reduced component weight) and the higher corrosion resistance, especially in case of "wet" CO_2. In the case of seals and gaskets, elastomeric seals are commonly used. There are likely to be cost benefits to be gained by adapting existing pipeline infrastructure used in the oil and gas industry for the transport of CO_2. Therefore, initial material selection may be based on materials with a long history of use in the oil and gas industry. However, some polymers, such as EPDM, which are generally unsuitable for oil and gas applications may be suitable for CO_2 transport application (IEAGHG, 2010). Sealing is quite essential to maintain pressure in the CO_2 transport system and therefore retain efficiency; the risks associated with small leakages in CCS due to seal failure should be assessed and managed through the life of the infrastructure (Cooper and Barnett, 2014). Table 1 shows a non-exhaustive list of polymers that have been identified in the CCS value chain, including in which types of component these polymer materials can typically be found. The chemical environment, temperatures, pressures and deterioration/failure of the materials in the application is usually not reported, so although these materials have been identified as having been used in the past, this does not imply that they are most suitable materials for these applications. In addition, it should be noted that polymeric materials are not highly standardised and are very dependent on synthesis and processing history. Commercial grades are also typically compounded with a wide variety of additives to enhance their properties, make them easier to process and more resistance to degradation. The presence of different amounts and types of these additives means that their properties and chemical compatibility may

vary between suppliers. Therefore, the data captured in this review should be considered indicative of typical properties but not absolute.

4. Impact of CO_2 on polymeric materials of the CCS value chain

4.1. Elastomers

Seals based on elastomer materials such as EPDM, fluorinated elastomers and nitrile rubbers are reportedly used in CO_2 transport systems (Gale and Davison, 2004; IEAGHG, 2010), but most literature relates to supercritical CO_2. As mentioned above, CO_2 can affect the performance of elastomers in different ways such as due to swelling and additive extraction, but also due to RGD damages. The severity of these interactions is determined by the way in which CO_2 interacts with the elastomer on the chemical and structural scales, and the effects of filler materials which are typically used to reinforce elastomers. Many elastomers are copolymers of two or more different monomers, and the relative composition of the monomers will also affect the compatibility with CO_2. Therefore, it is clear that different grades of elastomers within the same material family may have different CO_2 compatibility and should be assessed separately. For example, NBR, which is a co-polymer of butadiene and (polar) acrylonitrile monomers, is reported to have different CO_2 solubility depending on the acrylonitrile content (Khawaja et al., 2017). Furthermore, the interactions generated by the association of polar groups with the permanent dipole of the CO_2 molecule can lead to significant increase in CO_2 uptake and therefore to higher volumetric dilation compared to some engineering thermoplastics (such as PTFE) (Briscoe and Zakaria, 1991). In the same publication, even larger volume relaxations (up to ca. 80 % volume change) are reported for a silicone rubber depending on the CO_2 dissolved in the polymer matrix.

Dubois et al. describe the CO_2 uptake of various elastomers EPDM, NBR, SBR, EVM, CR and IR at pressures between 5 and 15 MPa (50–150 bar) (Dubois et al., 2018). While the CO_2 absorption was determined to increase with pressure, the behaviour was not linear in any of the polymer systems measured. A linear relationship between the CO_2 absorbed within the polymer matrix and the consequently induced swelling is reported (Fig. 5). For EPDM, the effect of temperature was investigated, revealing that the amount of CO_2 absorbed decreased with increasing temperature.

Hertz (2012) reported the effect of CO_2 absorption at ~ 5 MPa (50 bar) on EPDM, HNBR, 3 types of FKM and 2 types of FEPM. The effect of polymer type, degree of crosslinking, carbon black loading and carbon black particle size were all reported (Hertz, 2012). The degree of swelling was approximately in the order of the list above, with EPDM swelling least, while the fluorinated polymers were reported to swell the most. Hertz also subsequently expanded this research to include different HNBRs (Hertz, 2014), which is particularly relevant since HNBR is one of the most common elastomers used in the oil and gas industry due its combination of relative low cost and good chemical resistance to many organic liquids. Since fillers such as carbon black are assumed to not absorb CO_2, the amount of fillers has two main effects: firstly, polymers with high loading of filler have less polymer per unit mass and therefore would be expected to absorb less CO_2. Secondly, the filler acts as a physical barrier to gas diffusion increasing the tortuosity of the diffusion pathways. The aspect ratio (non-circularity) of fillers strongly influences this, as oriented flat platelets act as much better barriers to gas diffusion than fibres or spherical particles.

Schrittesser and co-workers investigated the effect of various operating parameters on the RGD damage resistance of an HNBR elastomer with a 36 % content of acrylonitrile (Schrittesser et al., 2016). Although the operating temperature (70–110 °C) is reported to have a limited effect, the CO_2 content in the gaseous phase is showed to determine a much larger volume increase when comparing the effects of exposing the materials to CO_2 or methane. Fig. 6 clearly shows that the effect is observed both in the pressurization and in the depressurization phase,
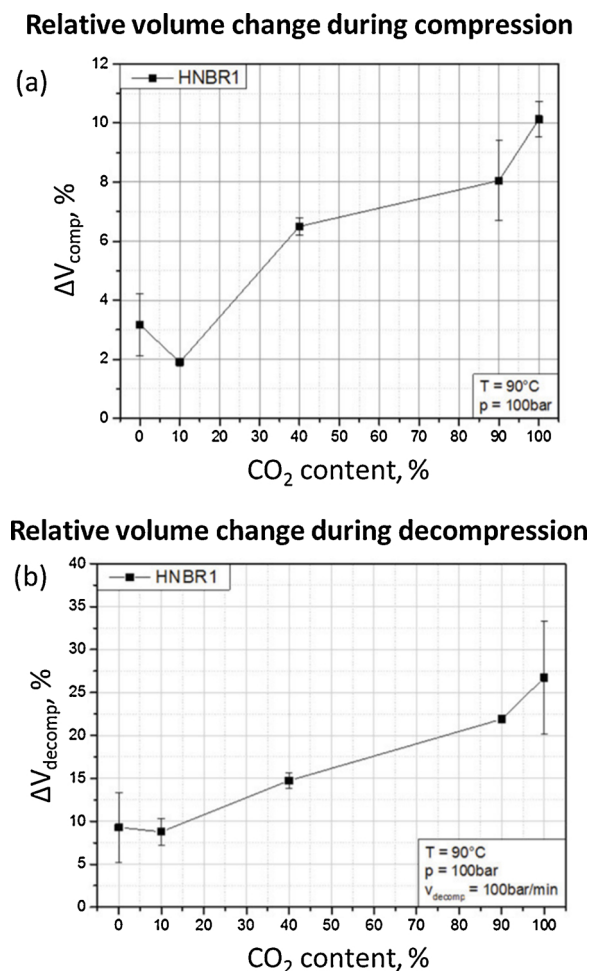
Relative volume change during compression

(a)

Relative volume change during decompression

(b)

Fig. 6. Volume increase during compression (a) and decompression (b) of HNBR at different CO_2 concentrations in the gaseous phase. Adapted from (Schrittesser et al., 2016) with permission from Elsevier.

mainly due to the higher solubility of CO_2 compared to methane. A 3-fold increase is observed in both cases. Furthermore, in the case of 100 % CO_2, the volume expansion upon RGD was observed to be proportional to the gas decompression rate, reaching a maximum increment of 50 % at 100 bar/min and 150 bar (saturation pressure).

Davies et al. reported the effect of CO_2 absorption on the tensile strength of 3 undisclosed fluorinated rubber compounds, 2 nitrile rubber compounds and a silicone rubber at 4 MPa (40 bar) (Davies et al., 1999). In all elastomers, significant reductions in stiffness, strength (< 50 %) and elongation at failure were reported. Control tests with air or nitrogen (which do not swell the polymers) under the same pressure did not result in significant changes in the mechanical performance, demonstrating the general weakening effect specifically due to CO_2 absorption.

Daou et al. (2014) reported a comprehensive study on the effect of elastomer exposure to wet-supercritical CO_2 and brine saturated CO_2 on elastomers, covering HNBR, NBR, FKM, EPDM, PTFE and also ACM (polyacrylic rubber), TFE/P (tetrafluoroethylene/propylene). The authors used two different methods for the investigation: exposure of the sample to the test conditions in a closed autoclave for 2 months and direct observation of the behaviour during exposure by means of a "visio-cell" equipped with a high-resolution camera. The results showed that several elastomers appeared to be relatively stable during the 2 months period, showing swelling not larger than 10 %, except for FKM and ACM, which showed large uptake and dilation upon exposure. Interestingly, they observed that the swelling did not always

corresponded to large CO_2 uptake (e.g., HNBR), but this is possibly related to the CO_2 desorption happening during the autoclave depressurization. To avoid damage, this step was performed slowly, significantly affecting the sorption/desorption behaviour of the polymer matrices. The visio-cell offered the possibility to observed real-time dilation of polymer particles (about 200 μm size) upon exposure to the supercritical CO_2 conditions. As results of this investigation, FKM and HNBR showed a quite large swelling, whereas PTFE and EPDM were found to show limited dilation, representing a valuable option as soft materials for supercritical CO_2 applications. For all the investigated materials, swelling was reported to happen quite quickly (normally within the first 24 h).

Abas et al. (2014) reported the exposure of different fluorinated elastomers (type 1 and 2 FKMs and a FFKM) to CO_2 at 150 bar and 80 °C, with the addition of 5000 ppm water. Type 1 and 2 FKM are similar elastomers but have some variations in composition and different total fluorine contents. After 2 weeks exposure and decompression, significant swelling and changes in hardness were reported in the type 2 FKM, and smaller changes in hardness and minor swelling in the type 1 FKM and FFKM. This demonstrates the fact that even subtle changes in the material composition can influence how elastomers are affected by CO_2 exposure.

The dispersion of inorganic phases within the elastomer matrix has also been proposed as method to improve the performance and stability in presence of pressurized CO_2. Chen et al. (2017) embedded pristine and surface-modified carbon nanotubes (CNTs) into a HNBR and a FKM matrix and evaluated the material response in terms of mass transport (solubility and diffusivity) and RGD when exposed to supercritical and liquid subcritical CO_2. It was reported that the CO_2 diffusivity is significantly affected by the amount of carbon black present in the HNBR composition, whereas a negligible influence is reported for the CO_2 solubility. For both HNBR and FKM, the presence of CNTs led to a significant increase of hardness, as it was expected due to the CNTs properties. In the case of HNBR, the presence of CNTs led to a minor increase in CO_2 diffusivity (especially for the functionalized CNTs) and solubility, and to a lower volume swelling, possibly due to the increased hardness. In the case of FKM, the inclusion of CNTs led to a reduction of both CO_2 diffusivity and solubility: the authors proposed that CNTs might have a confinement effect on the polymer matrix, limiting the CO_2-induced swelling, although no data on volume variations were reported. Tests targeting RGD resistance proved that CNTs are very effective in improving the performance of HNBR. Improvements were observed also for FKM, but the samples were not able to pass the designed tests. In another recent study, expanded graphite has been used as inorganic phase to reinforce FKM and HNBR, when exposed to high pressure CO_2 (Lainé et al., 2019). Compression of the pristine material up to 6 MPa showed that HNBR is negligibly affected by the presence of CO_2, even upon decompression and independently from the operating temperature (tests were performed at 60 and 130 °C). Different results are obtained for FKM, where the compression rigidity decreases at higher pressure and the memory of the pressurized phase is retained even after decompression. Unlike in the previous case, the inclusion of the inorganic phase lowered the materials' performance compared to the pristine case. For HNBR, the initial properties were retained only after decompression from 2 MPa (at 4 and 6 MPa the loss in stiffness is significant), whereas in the case of FKM, the compression after desorption showed that the material was seriously damaged. Visual inspection revealed that blistering and cracking were the main causes for the observed behaviour.

As shown in Table 1, different elastomers have different lower application temperatures, mainly governed by the glass transition temperature, T_g, below which seals are stiffer and more likely to leak (Akulichev et al., 2018). Therefore, the chemical compatibility of elastomers must be considered together with the ability of the elastomer to perform at the lower extremes of temperature expected (> −50 °C). A recent study (Shafiq et al., 2018) exploring the

blowdown of cryo-compressed vessel for CO_2 transport showed that despite the moderate operating pressure, a fast depressurization can lead to a drastic drop of the fluid temperature. As shown in Fig. 7, depending on the orifice of the valve (i.e., on the depressurization rate), the temperature of the fluid may decrease from $-40\ °C$ to below $-70\ °C$, reaching operating temperatures that are below the gas transition temperature of all the elastomers reported in Table 1.

4.2. Engineering thermoplastics

As shown in Table 1, engineering thermoplastics such as polyethylene and polypropylene may also be used in some applications which have contact with CO_2. As with elastomers described in the previous section, the CO_2 absorption behaviour of different thermoplastics is also dependent on factors such as the type of polymer, crystallinity (Shieh et al., 1996a), density and the presence of fillers. The majority of engineering thermoplastics which require high toughness in application are used above T_g, and so the T_g of thermoplastics influences the usage temperature. Nevertheless, some thermoplastics have T_g well above ambient temperature (for example, PEEK which has a T_g of ca. 145 °C, see Table 1) and so are commonly used below T_g. Therefore, in the case of thermoplastics, T_g is not always a limiting temperature for the material usage, depending on the requirements of the particular application. This is in contrast to elastomers which need to be used above T_g to have the required sealing properties, since these are intrinsically related to their rubbery behaviour in typical operating conditions. For example, PE has more limited applications at higher temperatures compared to PP, because of PEs relatively low melting temperature (T_m) (T_m of PE: 120 – 140 °C, T_m of PP: 165 – 175 °C). However, PE remains much tougher at lower temperatures than PP because of PE's lower T_g (T_g of PE: ca. -115 to -135 °C; T_g of PP: 0 to -25 °C). As well as mechanical properties, the difference in molecular mobility seen above and below T_g will also affect CO_2 compatibility, as mentioned previously. It is common practice to modify polymers, for example by copolymerizing or blending polymers, to achieve the required property for an application. In this case, the effect of CO_2 on the each of the constituent polymers may or may not reflect the effect of CO_2 on the modified materials. The effect of CO_2 of some engineering thermoplastics below T_g has also been reported (Abas et al., 2014; Bos et al., 1999).

It is expected that most engineering thermoplastics would also swell to some degree in dense phase CO_2 (DNV, 2009), and swelling data for polymers such as PE (Areerat et al., 2002; Sarrasin et al., 2015; Sawan et al., 1994), PP (Heinrich et al., 2009; Sawan et al., 1994) (Champeau et al., 2014), PET (Eggers, 2006; Sawan et al., 1994; von Schnitzler and Eggers, 1999), PVC (Sawan et al., 1994) and PTFE (Bonavoglia et al., 2006a; Sawan et al., 1994) have been reported. As described earlier, polar polymers (such as PMMA) would be expected to have a greater affinity to CO_2 and therefore exhibit greater CO_2 absorption and even risk of dissolution compared to non-polar polymers such as PE (Jiménez et al., 2007; Kazarian et al., 1996). The mechanical properties of some engineering thermoplastics and elastomers have been reported in literature after exposure to CO_2 at different pressures and temperatures for different durations. Jiménez et al. reported the exposure of HDPE, PTFE and a PA at 6.5 MPa and ambient temperatures (Fig. 8) and these polymers showed small weight changes due to CO_2 absorption (< 1 %) (Jiménez et al., 2007). These polymers are all semi-crystalline, and as described earlier lower CO_2 sorption would be expected in semi-crystalline polymers compared to completely amorphous polymers. No significant changes in tensile strength were reported (unlike for some polar polymers such as ABS, PC and PVC). There were also no significant changes in tensile stiffness for HDPE, PTFE or PA, although the standard deviation of the results was greater and so the results are less certain than those for tensile strength. PVC (which is typically toughened by plasticizers) showed an increase in stiffness and decrease in tensile strength, as would be expected if the CO_2 had extracted the

plasticizer additives. It should be noted that this study used a single cycle of CO_2 exposure, which may be indicative but not necessarily the same as the behaviour that might be expected after many more exposure cycles, or longer exposure times. Sawan et al. reported the changes in tensile properties of several polymers following exposure to CO_2 at different pressures and temperatures (Sawan et al., 1994). Here, the tensile properties of 20 different polymers - some amorphous (e.g. ABS and polycarbonate) and some semicrystalline (e.g. HDPE, PP, and PTFE) - were reported, together with changes in sample mass after exposure. Kim et al. (Kim et al., 2019) reported decreases in tensile strength and an increase in impact resistance of amorphous PET after exposure to CO_2 attributed to volumetric swelling and therefore reduction in network density of the polymer. Pasricha et al. (2005) reported on the effect of CO_2 exposure on the stiffness and creep resistance of polycarbonate (also amorphous). Here, the authors report a large decrease in stiffness after exposure to CO_2, which they describe as being analogous to testing the stiffness at a higher temperature. The authors also noted that the creep compliance is affected by CO_2 absorption and interestingly is still affected even after the CO_2 has been desorbed from the sample, suggesting a permanent change in the material due to the CO_2 exposure. Bao et al. (2011) report the use of super critical CO_2 exposure as an impact strength enhancing treatment to permanently change the morphology of injection moulded semicrystalline PP components. During the CO_2 exposure, the increase in free volume due to CO_2 swelling facilitates the recrystallisation of the PP, leading to a dramatic increase in impact resistance and although not reported here, it is likely that other mechanical properties would also be affected by this change in morphology. This illustrates how CO_2 swelling can lead to permanent changes in the properties of polymers, in addition to the transient changes in properties due to the swelling itself.

The absorption of CO_2 is also affected by the polarity of the molecules in a polymer; polyamide (PA) molecules are quite polar (due to the presence of carbonyl and amide groups), but the absorption of CO_2 is reported to be lower than would be expected. This is partly due to the crystallinity of the structure but is also likely due to the intermolecular hydrogen bonding present. The hydrogen bonding between neighbouring carbonyl and amide groups is reported to make them less available for interaction with CO_2 (Kazarian et al., 1996).

Engineering thermoplastics are of particular interest for the production of flexible pipes that can be applied in subsea operations (Fergestad and Løtveit, 2014). As shown in Fig. 9, an internal polymer liner is used to contain the fluid to be transported, whereas multiple metal armouring layers provide the required mechanical strength. Wang et al. (Wang et al., 2013) investigated the use of peroxide crosslinked PE (XLPE) and PVDF as potential liner materials in flexible piping for CO_2 application (operating conditions: T = 90 °C, P up to 345 bar). It should be highlighted that the crosslinking in the XLPE means that they are not actually thermoplastics, although some
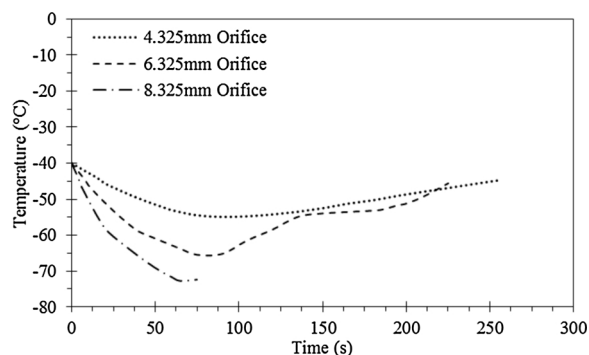
Fig. 7. Temperature drop due to the blowdown of a cryo-compressed vessel (initial pressure 40 bar, gas composition: 82.4 mol% CO_2, 15.3 mol% N_2, 2.3 mol% H_2S) as reported by (Shafiq et al., 2018).
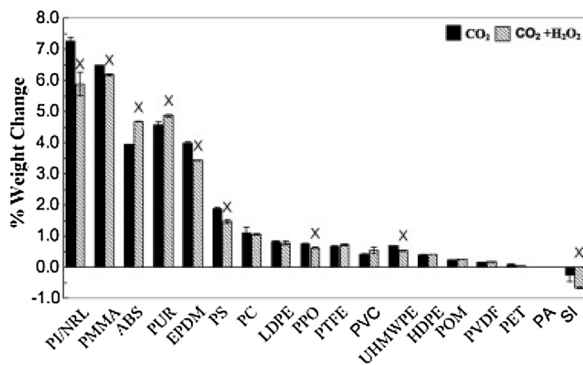
Fig. 8. CO_2 sorption in different polymeric materials at 6.5 MPa. Reprinted from (Jiménez et al., 2007) with the permission from Elsevier.

1) Stainless steel carcass
2) Polymer fluid barrier
3) Carbon steel pressure armour
4) Anti wear / birdcaging tapes
5) Carbon steel tensile armour
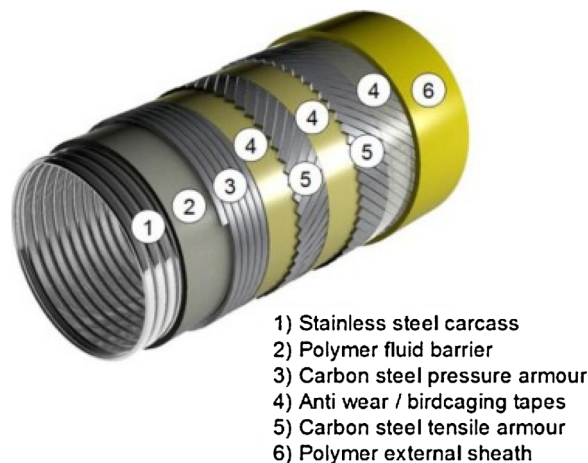6) Polymer external sheath

Fig. 9. Cross-section of a typical unbonded flexible pipe Reprinted from (Cornacchia et al., 2019) with the permission from Elsevier.

research on XLPE will still be included in this section. Solubility tests showed that the CO_2 uptake in XLPE (up to 300 bar) and PVDF (up to 150 bar) was deactivated at higher temperature, with the extent of variation been larger in case of XLPE than in PVDF. Rapid gas decompression was also investigated, showing that PVDF is negligibly affected by blistering at moderate pressure (100 bar, 90 °C), but the irreversible effects appear in the high-pressure range (300 bar, 90 °C), making the material unsuitable for multiple pressurisation cycles in

these operating conditions. No blistering was observed in XLPE up to 650 bar (at 90 °C) (Rubin and Wang, 2012). The authors also performed long-term (52 weeks, 100 bar, 90 °C) stability tests: in the case of PVDF, a loss in the strain at break was observed, whereas negligible variations were reported for the XLPE. Finally, gas permeability tests were performed using supercritical CO_2 as feed gas. For both PVDF (up to 150 bar) and XLPE (up to 650 bar), the CO_2 permeability was observed to increase with temperature (activated diffusion). Interestingly, opposite effects on the permeation behaviour were observed at increasing pressure: increase in the case of PVDF (possibly due to swelling), decrease in the case of XLPE (possibly due to free volume compaction). According to the results, XLPE is the most suitable candidate for high pressure applications, whereas PVDF can be suitable for more moderate CO_2 pressure. A 2013 report from The IEA Greenhouse Gas R&D Programme on CO_2 pipeline infrastructure describes PP as well as PE as potential liner materials for metallic pipes for CO_2 transport (Global CCS Institute, G., 2014).

Bonavoglia et al. (2006b) investigated the effect of absorption of CO_2 under supercritical conditions (up to 200 bar) in PTFE, PVDF and a PTFE random copolymer (TFE-PFMVE, tetrafluoroethylene–perfluoromethylvinylether). For PTFE and its random copolymer it was found that the dilation was up to 15 %, whereas higher values (up to 25 %) were observed in the case of PVDF. For all the investigated materials the dilation was found to increase with temperature for a given CO_2 concentration in the polymer matrix.

5. Impact of impurities on polymeric materials of the CCS value chain

So far, the general effects of CO_2 on polymeric materials has been considered but, in reality, the purity of the CO_2 collected at the emission site will be between 95 and 99 vol%. The impurities can be expected in different amounts depending on the CO_2 production process and on the type of capture system retrofitted (de Visser et al., 2008; Martynov et al., 2016; Neele et al., 2017). An example of the type of impurities for various sources is shown in Table 2, as reported by Neele et al., 2017. Apart from traces of common gases (N_2, CH_4, H_2, Ar, O_2), the CO_2 can contain also traces of NO_x, SO_x, H_2S, NH_3 and amines. According to the DNV-GL Recommended Practice, aldehydes may also be present (DNVGL, 2017). Therefore, while the majority of literature focuses on the effect of pure CO_2 on materials, this does not fully describe the effects that may occur in real applications.

Some authors have described different aspects of the presence of impurities on CO_2 transport and storage (Coquelet et al., 2017; Huh et al., 2011; Neele et al., 2017; Wang et al., 2011), but little work has

Table 2

Examples of highest level of impurities contained in captured CO_2 emissions from different sites (Neele et al., 2017).

Source Type	Coal-fired power plant				Natural gas processing	Synthetic gas processing
Capture technology	Amine-based absorption	Ammonia-based absorption	Selexol-based absorption	Oxyfuel combustion	Amine-based absorption	Rectisol-based absorption
Gaseous stream concentration [a]						
CO_2	99.8 %	99.8 %	98.2 %	95.3 %	95.0 %	96.7 %
N_2	2000	2000	6000	2.5 %	5000	30
O_2	200	200	1	1.6 %	–	5
Ar	100	100	500	6000	–	–
NO_x	50	50	–	100	–	–
SO_x	10	10	–	100	–	–
CO	10	10	400	50	–	1000
H_2S	–	–	100	–	200	9000
H_2	–	–	1.0 %	–	–	500
CH_4	–	–	1000	–	4.0 %	7000
C_2+	–	–	–	–	5000	1.5 %
NH_3	1	100	–	–	–	–
Amine	1	–	–	–	–	–

[a] the values are reported in mol% (where indicated) or in ppmv. Water content not included. Desulphurisation included.

been published on how the impurities may impact material compatibility, especially for polymer materials. Scientific investigation appeared to be limited to metal pipelines (Halseid et al., 2014; Patchigolla and Oakey, 2013; Patchigolla et al., 2014; Rütters et al., 2016). In the project "MATTRAN" (Race et al., 2009), the effect of impurities (mainly sulphur components) was thoroughly investigated for CO_2 pipelines. Among the publications listed within that project, the research team reported the investigation of soft materials (polymeric seals such as neoprene, fluorocarbon, ethylene propylene rubber and Buna N), although no results of the characterisation of those materials were presented (Patchigolla and Oakey, 2013).

Nevertheless, the effect of larger concentration of impurities components on soft materials can be considered a good guideline for the materials selection. In particular, data observed at higher impurities concentration in short time may be considered to give a good approximation of long-term exposure to trace amounts of impurities. CO_2-induced swelling or plasticization phenomena can also increase the uptake and its kinetics, accelerating the effects. For example, if a polymer is swollen by the presence of high-pressure CO_2, the impurities in the gas stream would be expected to diffuse faster through the swollen polymer compared to its non-swollen state. Therefore, in this section we

report some literature findings about compatibility of polymeric materials of interest and the impurities components mentioned in Table 2.

Chemical compatibility tables of plastics with respect to various chemicals can be obtained from several polymer producers/suppliers, and the results reported are typically very similar. In Table 3, the compatibility of various soft materials of interest is reported according to the information available on the internet from a selection of different plastic producers. Therefore, Table 3 gives an indication of compatibility of some common polymers with very concentrated chemicals: green indicates that good compatibility (or little interaction between the concentrated chemical and the polymer) would be expected, orange indicates poor compatibility (or some interaction between the concentrated chemical and the polymer) would be expected, while red indicates a strong reaction between the concentrated chemical and the polymer would be expected, which would mean that this combination could be unsuitable. Where conflicting data were found in different sources for the different material groups, the worse of the reported compatibilities was used in Table 3. If good compatibility between the polymer and very concentrated chemicals is detected, this indicates that lower concentrations also may be compatible. If poor compatibility between the polymer and very concentrated chemicals is detected, it

Table 3

Typical stability of some polymer materials with respect to various contaminants. Data combined from a selection of materials suppliers (Ingersoll Rand, 2019) (ChemlinePlastics, 2018), (Nylacast, 2018) (ISM, 2019) (IPEX, 2019) (Plastics Pipe Institute, 2019) (Thermo Scientific, 2019) (Marco Rubber and Plastics, 2019). Green indicates good compatibility with the concentrated chemical; orange indicates poor compatibility with the concentrated chemical and red indicates that significant interactions with the concentrated chemical are expected and therefore this combination could be unsuitable. The sources were chosen arbitrarily from commercially available literature, and the results must be considered as indicative rather than absolute.

Component	Conc. (mol%)	HDPE	PP	PA12	PTFE	PVDF	Fluoro-elastomer	EPDM	NBR	SBR	IR	CR
CH₄	100	green	green	-	green	green	green	green	green	orange	green	orange
CO	100	green	green	-	green	green	green	orange	green	green	green	orange
H₂	100	green	green	green/orange	green	green	green	green	green	green	green	green
H₂S gas (dry)	100	green	green	green/orange	green	green	green	green	red	green	orange	orange
NH₃ gas	100	green	green	red	green	red	red	green	green	green	green	green
Water	100	green	green	green	green	green	green	green	green	green	green	orange
SOx												
SO₂	100	green	green	-	green	green	orange	green	red	red	red	orange
SO₃	100	red	red	-	orange	red	-	-	-	red	orange	red
NOx												
N₂O	100	green	green	-	green	green	-	green	green	green	green	green
NO₂	100	green	green	-	green	green	green	green	green	green	green	green
Amines												
Butylamine	100	green	red	-	green	orange	green	red	green	red	red	red
Dibutylamine	100	-	-	-	green	-	-	-	-	red	red	red
Diethylamine	100	orange	green	-	green	red	orange	red	green	red	orange	red
Diethylenamine	100	-	orange	-	green	-	-	-	-	-	-	-
Diethylenetriamine	100	red	red	-	green	-	-	-	-	-	-	-
Dimethylamine	100	-	green	-	green	red	red	green	red	orange	green	green
Monoethanolamine	100	-	-	-	green	-	-	green	red	orange	green	green
Triethanolamine	100	orange	green	-	green	green	green	green	red	green	green	green
Triethylamine	100	green	red	-	green	orange	green	green	red	orange	green	green
Methylamine	100	red	orange	-	green	green	green	green	green	green	green	green
Aldehydes												
Acetaldehyde	100	green	green	green	green	red	orange	green	green	green	green	orange
Acetaldehyde	40	green	green	green	green	-	orange	orange	red	green	-	-
Formaldehyde	35	green	green	orange	green	green	green	orange	orange	orange	orange	orange
Formaldehyde	50	-	green	-	green	-	green	green	green	-	-	-

NOTE: an increase in temperature is typically corresponding to a decrease in stability (higher diffusion, higher reaction kinetics). However, the effect of temperature on stability can be significantly different, and each case should be carefully investigated depending on the specific need.

cannot be concluded that lower concentrations may be more tolerated by the materials over longer timescales, because the thresholds required for the exposure chemicals to attack the polymers are unknown. Such tables typically describe the compatibility with only one chemical which may or may not be indicative of the effects of combinations of these chemicals; the compatibility of materials with a CO_2 stream containing the ppm levels of expected impurities listed in Table 2 is difficult to predict from these data. It is also important to note that such tables give good insight into the expected stability of materials, but the classification is strongly dependent on the performance criteria (frequently not clearly explained by the sources). Therefore, material compatibility should always be tested in the worst-case combinations of conditions expected, with appropriate failure criteria defined by the application.

According to Table 3, one of the most critical situations is represented by the presence of SO_3, since many of the reported plastics are shown to have a poor stability (with the exception of PTFE and some other highly fluorinated polymers). PP and PTFE are reported to have good stability with most of the other impurities, with PTFE showing the best performance. Many of the elastomers are reported to have poor stability towards amines and aldehydes. Among the elastomers considered in the table, EPDM shows the best performance, whereas NBR is reported to be characterized by less stable behaviour. The presence of inert (N_2, Ar) or flammable (H_2, CH_4) gases in ppm amount is expected to have a negligible impact on the performance of the polymeric materials, in view of their low reactivity and solubility in polymer matrices. O_2 can lead to polymer oxidation, but this is normally managed by antioxidants in exposure conditions at elevated temperatures, and very high temperatures are outside the boundaries of typical CO_2 transport operations.

In the following subsections, the main effects associated with each impurity possibly present in the CO_2 gaseous stream are describe according to literature.

5.1. Water

According to Table 3, water alone is expected to have negligible influence on the performance of the materials of interest for the application, although some polymers such as polyamides are known to undergo hydrolysis in some conditions. Nevertheless, water plays a critical role in the corrosion behaviour. For this reason the free-water content in dense phase CO_2 is kept as low as possible (Xiang et al., 2017). Water may react with CO_2 to form carbonic acid (Dillow et al., 1999), which although considered relatively weak, may combine with other acids present and attack polymer materials (Halseid et al., 2014). Examples of other acids that may be expected are nitric and sulphuric acid, resulting from the reaction of SO_x and NO_x with water (Cole et al., 2011; Sim et al., 2013).

5.2. H$_2$S

H_2S is a condensable component, and therefore it can be absorbed in organic material to a significant extent. However, perfluoropolymers (mainly PTFE copolymers) show unexpectedly low H_2S permeability compared to non-fluorinated polymers (Merkel and Toy, 2006). Solubility measurements clearly highlight that H_2S solubility in this type of materials is unexpectedly low, especially compared to CO_2, which has a lower condensability compared to H_2S. According to the study, this behaviour is possibly associated to unfavourable interactions of H_2S with the fluorine groups present in the polymer structure.

At concentrations below 2000 ppm most of the elastomers are expected to be stable in H_2S (Table 3). However, it should be taken into account that the H_2S can influence the degradation temperature: fluorinated elastomers can undergo degradation via hydrolysis at elevated (> 500 °C) temperature, potentially releasing hydrofluoric acid. It is reported that the presence of H_2S can reduce this temperature

below 300 °C, in view of the more nucleophilic nature of the molecule with respect to water (Harwood, 1983). A particular case is represented by NBR (Ho, 2006), where H_2S can attack the acetonitrile groups, therefore NBR elastomers with low ACN content should be more stable than those with higher ACN content.

5.3. Aldehydes

Few data are available on the effect of aldehydes on the polymers mentioned in Table 1. A literature study (Aminabhavi and Munnolli, 1993) on aldehydes (*n*-Butaraldehyde, Benzaldehyde) confirms the data reported in Table 3 in terms of stability towards this class of components. In fact, EPDM shows the best performance (low sorption and diffusion of the aldehydes in the polymer matrix), whereas NBR was observed to absorb the largest amount, undergoing significant volume expansion. High sorption and relatively significant volume expansion were observed also for SBR and CR, suggesting that poor stability can be expected for those materials during long-term exposure. In the *Recommended practice from DNV-GL* it is indicated that in presence of water, aldehydes may form acids, generating a corrosive aqueous phase (DNVGL, 2017).

5.4. Amines and ammonia

Amines are reported to be able to induce crosslinking in some of the fluoroelastomers and they are used as such to increase their chemical resistance. The amine reactivity is related to the number of substituents of the H atoms surrounding the N, with the primary amines being the most reactive, followed by secondary and tertiary amines (Paciorek et al., 1960). The crosslinking is associated to a dehydrohalogenation reaction, followed by an addition to the centre of unsaturation. Crosslinking typically leads to an increase of the chemical resistance but also to stiffer materials, which can be problematic for elastomers used as seals or gaskets.

A recent study evaluated the effect of aqueous amines exposure in EPDM, natural rubber (NR), isobutylene isoprene rubber (IIR), SBR and PTFE, at 40 and 120 °C (Srisang et al., 2014). All the investigated elastomers showed a significant solvent uptake, with the effect being enhanced by temperature, but partially hindered at increasing the CO_2 loading (possibly due to a lower amine availability). FTIR spectroscopy analysis highlighted that SBR and NR also underwent chemical modification due to reactions with amines, while a negligible effect on the spectra was observed for EPDM and IIR. On the contrary, PTFE exhibited excellent chemical stability: compared to EPDM and IIR, PTFE retained its hardness and tensile strength even upon exposure concentrated amine solution at high temperature (Srisang et al., 2014). Good amine compatibility of PTFE was also reported in other studies, where in addition to the primary amines, secondary and tertiary amines were also considered (Ansaloni et al., 2016). Anhydrous ammonia testing on EPDM and PTFE showed negligible effect of ammonia on both materials (Benner and Schweickart, 1992).

5.5. SO$_x$ and NO$_x$

SO_x (sulphur oxides) and NO_x (nitrogen oxides) can be problematic as they can lead to the formation of acids in presence of water. For example, in gaseous streams with the presence of traces of SO_3 and water, if condensation occurs the first droplets can be highly concentrated in the acid content, possibly determining the corrosion of the materials they are in contact with. A similar situation can be encountered when NO_x is present in the gaseous CO_2 stream. This means that even very low concentrations in the entire systems may result in high concentrations locally (e.g. in a droplet or mist) if the pressure and temperature are varied along the value chain (Halseid et al., 2014).

Resistance to sulfuric and nitric acid can be problematic for several elastomers (such as EPDM, NBR, SBR, natural rubber, CR) with the

exception of CSM and FKM, with the latter being the relatively stable among elastomers. Polypropylene and polyethylene are able to offer some stability towards dilute sulfuric and nitric acid, whereas PTFE has excellent stability towards both components (Schweitzer, 2006), so these would be candidates for use in situations where low concentrations of NOx and SOx might be expected in the CO_2 stream.

6. Conclusions

Polymeric materials with suitable performance in the operating windows typical of the CO_2 transport process are required to ensure the deployment of CCS at the full scale. To maximize the transport efficiency, CO_2 must be transported as high-density fluid and, depending on the transport mode (ships or pipelines), the polymer-based materials are expected to be exposed to conditions that are outside the traditional ranges used nowadays in most industries. Nevertheless, a thorough literature study on the polymers' types of interest showed that the existence of large gaps in knowledge base about the effects of highly concentrated CO_2 phases on polymer-based materials in conditions relevant for the CO_2 transport.

Table 4 shows a summary of the factors reported in literature which should be considered when selecting polymers for use in the CO_2 transport chain, as presented in this review paper. Since different authors have tested many different aspects of the CO_2 compatibility of these polymers under different operating temperatures, the validity of any extrapolation outside of the tested range should be carefully assessed on a case by case basis.

According to the available data, it can be concluded that, among elastomers used as gaskets and sealants, there is a wide range of factors to be considered during material selection. Fluorinated polymers which are commonly used in applications that require chemical resistance, may undergo significant volumetric swelling due to CO_2 sorption, even though they may not undergo significant chemical reactions. Some elastomers such as HNBR which are commonly used in the oil and gas industry should be carefully selected since their composition (for example the acrylonitrile content in HNBR) can significantly affect the CO_2 uptake and release upon rapid gas decompression scenarios. Furthermore, the high CO_2 concentrations with respect to current industrial conditions (e.g., in natural gas) may result in a stronger effect on these types of materials upon rapid decompression than seen today in applications in the oil and gas industry. In the case of engineering thermoplastics (employed in vessels and pipes), the presence of crystallinity may limit the CO_2 sorption/volumetric swelling within the polymer matrix compared to amorphous thermoplastics or elastomers.

Table 4

Summary of factors reported in literature which may influence material selection within the CO_2 transport chain for elastomers and engineering thermoplastics.

Polymer	Factors which may influence material selection within the CO_2 transport chain
Elastomers	
NBR, HNBR	Established use in Oil & Gas industry
	Relatively low cost
	Moderate CO_2 uptake and volumetric swelling
	Susceptible to chemical interaction with H_2S, SOx, amines, aldehydes
	The ACN content in the polymer affects the CO_2 solubility and the CO_2 diffusion during RGD
	Permanent reduction in mechanical properties reported after CO_2 exposure
	Tg above the CO_2 triple point
FKM, FFKM, FEPM	Excellent chemical resistance to most impurities
	High CO_2 uptake and volumetric swelling due to affinity of CO_2 to fluorine reported
	Permanent reduction in mechanical properties reported after CO_2 exposure
	Tg typically above cryo-compressed conditions
EPDM	Low CO_2 uptake and volumetric swelling
	Improved resistance to CO_2-induced RGD damages, due to fast degassing
	Susceptible to chemical interaction with amines
	Tg in the range of the CO_2 triple point
	Limited use in the Oil & Gas industry due to poor compatibility towards hydrocarbons
SBR	Moderate CO_2 uptake and volumetric swelling
	Susceptible to chemical interaction with SOx, amines, aldehydes
	Tg in the range of the CO_2 triple point
IR	Low CO_2 uptake and volumetric swelling
	Susceptible to chemical interaction with SOx, amines, aldehydes
	Tg below the CO_2 triple point
CR	Moderate CO_2 uptake and volumetric swelling
	Susceptible to chemical interaction with SOx, amines, aldehydes
	Tg above the CO_2 triple point
Engineering Thermoplastics	
PTFE	Excellent chemical resistance to most impurities
	High CO_2 uptake among thermoplastics, due to affinity of CO_2 to fluorine
	Moderate CO_2 volumetric swelling
XLPE	Low CO_2 uptake and negligible volumetric swelling
	Good stability towards RGD damage reported
	CO_2 permeability decreases along with CO_2 pressure (compaction effect)
HDPE	Susceptible to chemical interaction with amines
	Moderate CO_2 uptake
PA	Low CO_2 uptake
	Susceptible to chemical interaction with H_2S, NH_3
PVDF	High CO_2 uptake among thermoplastics, due to affinity of CO_2 to fluorine
	High CO_2 volumetric swelling
	Susceptible to chemical interaction with SOx, amines, aldehydes
	Irreversible RGD damage at high pressure (300 bar) supercritical conditions reported
	CO_2 permeability increases with CO_2 pressure (plasticization effect)

The extracting power of liquid CO_2 is reported to remove additives such as plasticizers from polymers, resulting in changes in mechanical properties over time. As with fluorinated elastomers, the presence of fluorine groups in thermoplastics such as PTFE and PVDF appears to enhance the CO_2-philicity of the material. For example, the CO_2 permeability of PVDF was found to increase along with the operating pressure, due to CO_2-induced swelling. On the other hand, crosslinked PE shows promising performance for highly pressurized conditions.

In view of the analysis performed, the following open challenges have been identified:

- most of the literature data are reported for temperatures > 50 °C: the measurement of the properties of materials at lower temperatures (for example approaching the triple point, −54 °C) will also indicate how suitable materials are in environments which are more relevant to the CO_2 transport chain.
- the effect of pressure and temperature cycling on the materials should be investigated to understand how this may affect their mechanical stability. This cyclic loading would be expected during batch wise transport of CO_2 (e.g. required by the ship-mode transport operating at temperatures close to the T_g of the many polymers of interest) and is therefore an important factor which affects the expected lifetime of a polymer component;
- under cryo-compressed conditions some absorption of CO_2 in the polymer is expected. As with all compressed gas scenarios in contact with polymer materials, there is a risk of rapid gas decompression damage during depressurisation, and therefore the risks associated with RGD damage due to absorbed dense phase CO_2 should be assessed;
- some polymers show great potential to be used in the CO_2 transport chain (such as PE and EPDM). However, many of the polymer materials reported in literature appear to be based on history of use in the oil and gas industry rather than being optimised for use in contact with dense or liquid phase CO_2. Therefore, there is potential for material optimisation, but this requires further application-specific investigations to be conducted;
- the gap of knowledge about the influence of impurities present in dense or liquid phase CO_2 on the performance of polymeric materials (both elastomers and thermoplastics) must be investigated further to ensure safe and reliable operations.

Addressing these open challenges will lead to progress in closing the knowledge gaps identified in this paper, allowing more informed polymeric material selection within the CO_2 transport chain.

Declaration of Competing Interest

The authors declare that they have no known competing financial interests or personal relationships that could have appeared to influence the work reported in this paper.

Acknowledgements

References

Abas, A.Z., Mohammed Nor, A., Suhor, M.F., Mat, S., 2014. ₂Non-metallic materials in supercritical CO systems. In: Offshore Technology Conference-Asia. Offshore Technology Conference, Kuala Lumpur. Malaysia. pp. 4.

Akulichev, A.G., Echtermeyer, A.T., Persson, B.N.J., 2018. Interfacial leakage of elastomer seals at low temperatures. Int. J. Press. Vessel. Pip. 160, 14–23.

Alessi, P., Cortesi, A., Kikic, I., Vecchione, F., 2003. Plasticization of polymers with supercritical carbon dioxide: experimental determination of glass-transition temperatures. J. Appl. Polym. Sci. 88, 2189–2193.

Aminabhavi, T.M., Munnolli, R.S., 1993. Sorption and diffusion of aldehydes and ketones into elastomers. Polym. Int. 32, 61–70.

Ansaloni, L., Arif, A., Ciftja, A.F., Knuutila, H.K., Deng, L., 2016. Development of membrane contactors using phase change solvents for CO₂ capture: material compatibility study. Ind. Eng. Chem. Res. 55, 13102–13113.

Areerat, S., Hayata, Y., Katsumoto, R., Kegasawa, T., Egami, H., Ohshima, M., 2002. Solubility of carbon dioxide in polyethylene/titanium dioxide composite under high pressure and temperature. J. Appl. Polym. Sci. 86, 282–288.

Aspelund, A., Mølnvik, M.J., De Koeijer, G., 2006. Ship transport of CO₂: technical solutions and analysis of costs, energy utilization, exergy efficiency and CO₂ emissions. Chem. Eng. Res. Des. 84, 847–855.

Aursand, E., Aursand, P., Hammer, M., Lund, H., 2016. The influence of CO₂ mixture composition and equations of state on simulations of transient pipeline decompression. Int. J. Greenh. Gas Control. 54, 599–609.

Bao, J.-B., Liu, T., Zhao, L., Hu, G.-H., 2011. Carbon dioxide induced crystallization for toughening polypropylene. Ind. Eng. Chem. Res. 50, 9632–9641.

Barnes, P., 2001. Method of cleaning or purifying elastomers and elastomeric articles which are intended for medical or pharmaceutical use, EP0906361A1.

Belhadj-Ahmed, F., Badens, E., Llewellyn, P., Denoyel, R., Charbit, G., 2009. Impregnation of vitamin E acetate on silica mesoporous phases using supercritical carbon dioxide. J. Supercrit. Fluids 51, 278–286.

Benner, S., Schweickart, R., 1992. Compatibility testing with anhydrous ammonia. In: 33rd Structures, Structural Dynamics and Materials Conference Dallas. US.

Bonavoglia, B., Storti, G., Morbidelli, M., 2006a. Modeling of the sorption and swelling behavior of semicrystalline polymers in supercritical CO₂. Ind. Eng. Chem. Res. 45, 1183–1200.

Bonavoglia, B., Storti, G., Morbidelli, M., Rajendran, A., Mazzotti, M., 2006b. Sorption and swelling of semicrystalline polymers in supercritical CO₂. J. Polym. Sci. 44, 1531–1546.

Bos, A., Pünt, I.G.M., Wessling, M., Strathmann, H., 1999. CO₂-induced plasticization phenomena in glassy polymers. J. Memb. Sci. 155, 67–78.

Brachthäuser, K., Kleinrahm, R., Lösch, H.W., Wagner, W., 1993. Entwicklung eines neuen Dichte-meßverfahrens und Aufbau einer Hochtemperatur-Hochdruck-Dichtemeßanlage. VDI-Verl, Dusseldorf.

Briscoe, B.J., Savvas, T., Kelly, C.T., 1994. "Explosive decompression failure" of rubbers: a review of the origins of pneumatic stress induced rupture in elastomers. Rubber Chem. Technol. 67, 384–416.

Briscoe, B.J., Zakaria, S., 1991. Interaction of CO₂ gas with silicone elastomer at high ambient pressures. J. Polym. Sci. 29, 989–999.

Calleja, G., Jourdan, A., Ameduri, B., Habas, J.-P., 2013. Where is the glass transition temperature of poly(tetrafluoroethylene)? A new approach by dynamic rheometry and mechanical tests. Eur. Polym. J. 49, 2214–2222.

Champeau, M., Thomassin, J.M., Jérôme, C., Tassaing, T., 2014. In situ FTIR microspectroscopy to investigate polymeric fibers under supercritical carbon dioxide: CO₂ sorption and swelling measurements. J. Supercrit. Fluids 90, 44–52.

ChemlinePlastics, S., 2018. Chemical Resistance Guide. (accessed November 2018). https://www.chemline.com/media/Chemline-Plastics-chemical-resistance-guide.pdf.

Chen, X., Salem, H.A., Zonoz, R., 2017. CO₂ solubility and diffusivity and rapid gas decompression resistance of elastomers containing CNT. Rubber Chem. Technol. 90, 562–574.

Cole, I.S., Corrigan, P., Sim, S., Birbilis, N., 2011. Corrosion of pipelines used for CO₂ transport in CCS: is it a real problem? Int. J. Greenh. Gas Control. 5, 749–756.

Cooper, R., Barnett, J., 2014. Pipelines for transporting CO₂ in the UK. Energy Procedia 63, 2412–2431.

Coquelet, C., Stringari, P., Hajiw, M., Gonzalez, A., Pereira, L., Nazeri, M., Burgass, R., Chapoy, A., 2017. Transport of CO₂: presentation of new thermophysical property measurements and phase diagrams. Energy Procedia 114, 6844–6859.

Cornacchia, F., Liu, T., Bai, Y., Fantuzzi, N., 2019. Tensile strength of the unbonded flexible pipes. Compos. Struct. 218, 142–151.

Daou, F., de Miranda, C.R., de Oliveira, J.L., Engelke, B., Borman, C., Le Roy-Delage, S., Lungwitz, B., 2014. Swelling of elastomers in CO₂ environment: testing methodology and experimental data. In: SPE Latin America and Caribbean Petroleum Engineering Conference. Society of Petroleum Engineers. Maracaibo, Venezuela. pp. 16.

Davies, O.M., Arnold, J.C., Sulley, S., 1999. The mechanical properties of elastomers in high-pressure CO₂. J. Mater. Sci. 34, 417–422.

Davies, O.R., Lewis, A.L., Whitaker, M.J., Tai, H., Shakesheff, K.M., Howdle, S.M., 2008. Applications of supercritical CO2 in the fabrication of polymer systems for drug delivery and tissue engineering. Adv. Drug Deliv. Rev. 60, 373–387.

de Visser, E., Hendriks, C., Barrio, M., Mølnvik, M.J., de Koeijer, G., Liljemark, S., Le Gallo, Y., 2008. Dynamis CO₂ quality recommendations. Int. J. Greenh. Gas Control. 2, 478–484.

DeCrosta, M., Jagnandan, I., 1999. Method for Cleaning Elastomeric Articles.

Dillow, A.K., Dehghani, F., Hrkach, J.S., Foster, N.R., Langer, R., 1999. Bacterial inactivation by using near- and supercritical carbon dioxide. Proc. Natl. Acad. Sci. 96, 10344–10348.

DNV, 2009. DNV Report 2008-1993: Mapping of Potential HSE Issues Related to Large-scale Capture, Transport and Storage of CO₂.

DNVGL, 2017. Recommended Practice DNVGL-RP-F104: Design and Operation of Carbon Dioxide Pipelines.

Doroudiani, S., Park, C.B., Kortschot, M.T., 1996. Effect of the crystallinity and morphology on the microcellular foam structure of semicrystalline polymers. Polym. Eng. Sci. 36, 2645–2662.

Dubois, J., Grau, E., Tassaing, T., Dumon, M., 2018. On the CO₂ sorption and swelling of elastomers by supercritical CO₂ as studied by in situ high pressure FTIR microscopy.

J. Supercrit. Fluids 131, 150–156.

Dugstad, A., Halseid, M., Morland, B., 2013. Effect of SO_2 and NO_2 on corrosion and solid formation in dense phase CO_2 pipelines. Energy Procedia 37, 2877–2887.

Ebnesajjad, S., 2015. 17 - Chemical properties of fluoropolymers—polytetrafluoroethylene and polychlorotrifluoroethylene. In: Ebnesajjad, S. (Ed.), Fluoroplastics, second edition. William Andrew Publishing, Oxford, pp. 382–395.

Eggers, R., 2006. Sorption behaviour and swelling of polymers in a carbon dioxide atmosphere at transcritical conditions. In: 7th IIR Gustav Lorentzen Conference on Natural Working Fluids. Trondheim, Norway. May 28-31,2006.

Eldevik, F., Graver, B., Torbergsen, L.E., Saugerud, O.T., 2009. Development of a guideline for safe, reliable and cost efficient transmission of CO_2 in pipelines. Energy Procedia 1, 1579–1585.

Energy Institute London, 2010. Good Plant Design and Operation for Onshore Carbon Capture Installations and Onshore Pipelines in: Institute, G.C. (Ed.).

Equinor, Shell, Total, 2018. Northern Lights – Mottak Og Lagring Av CO2. Forslag Til Utredningsprogram for Konsekvensutredning, RE-PM673-00010. Equinor, Norway.

Fergestad, D., Løtveit, S.A., 2014. Handbook on Design and Operation of Flexible Pipes. Trondheim, Norway.

Gale, J., Davison, J., 2004. Transmission of CO_2—safety and economic considerations. Energy 29, 1319–1328.

Gassnova, Gassco, 2016. Mulighetsstudier Av Fullskala CO_2-håndtering I Norge. Olje- og energidepartementet, Norges Regjeringen.

Geske, J., Berghout, N., van den Broek, M., 2015a. Cost-effective balance between CO_2 vessel and pipeline transport. Part I – impact of optimally sized vessels and fleets. Int. J. Greenh. Gas Control. 36, 175–188.

Geske, J., Berghout, N., van den Broek, M., 2015b. Cost-effective balance between CO_2 vessel and pipeline transport: part II – design of multimodal CO_2 transport: the case of the West Mediterranean region. Int. J. Greenh. Gas Control. 33, 122–134.

Global CCS Institute, 2010. Corrosion and material selection in CCS systems, report nr. 2010/03. In: Institute, G.C. (Ed.), Carbon Capture. Use and storage (CCUS).

Global CCS Institute, G, 2014. CO_2 pipeline infrastructure. In: Institute, G.C. (Ed.), Carbon Capture. CO2 transport, Use and storage (CCUS).

Global CCS Institute, G, 2017. Challenges related to carbon transportation and storage – showstoppers for CCS? In: Institute, G.C. (Ed.), CO_2 Storage, CO_2 Transport.

Goos, E., Riedel, U., Zhao, L., Blum, L., 2011. Phase diagrams of CO_2 and CO_2–N_2 gas mixtures and their application in compression processes. Energy Procedia 4, 3778–3785.

Guo, X., Yan, X., Yu, J., Yang, Y., Zhang, Y., Chen, S., Mahgerefteh, H., Martynov, S., Collard, A., 2017. Pressure responses and phase transitions during the release of high pressure CO_2 from a large-scale pipeline. Energy 118, 1066–1078.

Guo, X., Yan, X., Yu, J., Zhang, Y., Chen, S., Mahgerefteh, H., Martynov, S., Collard, A., Proust, C., 2016. Pressure response and phase transition in supercritical CO_2 releases from a large-scale pipeline. Appl. Energy 178, 189–197.

Halseid, M., Dugstad, A., Morland, B., 2014. Corrosion and bulk phase reactions in CO_2 transport pipelines with impurities: review of recent published studies. Energy Procedia 63, 2557–2569.

Hansen, C.M., 2004. 50 Years with solubility parameters—past and future. Prog. Org. Coat. 51, 77–84.

Harwood, H., 1983. Ethylene-Propylene-Diene Monomer (EPDM) and Fluorocarbon (FKM) Elastomers in the Geothermal Environment.

Haug, J.K., Stigson, P., 2016. Local acceptance and communication as crucial elements for realizing CCS in the nordic region. Energy Procedia 86, 315–323.

Heinrich, H., Jaeger, P., Eggers, R., 2009. Diffusion Von Gasen und Gasgemischen in Polymere unter hohen drücken. Chemie Ingenieur Tech. 81, 1607–1611.

Hertz, D.L., 2012. Elastomers in CO_2. High Performance Elastomers & Polymers for Oil & Gas 2012, Aberdeen, UK.

Hertz, D.L., 2014. HNBR in CO_2. High Performance Elastomers & Polymers for Oil & Gas 2014, Aberdeen, UK.

Ho, E., 2006. Elastomeric Seals for Rapid Gas Decompression Applications in High pressure Services. BHR Group Limited for the Health and Safety Executive, UK.

Huang, N., Day, G., Yang, X., Drake, H., Zhou, H.-C., 2017. Engineering porous organic polymers for carbon dioxide capture. Sci. China Chem. 60, 1007–1014.

Huh, C., Kang, S.-G., Cho, M.-I., Baek, J.-H., 2011. Effect of water and nitrogen impurities on CO_2 pipeline transport for geological storage. Energy Procedia 4, 2214–2221.

IEAGHG, 2010. Corrosion and Material Selection in CCS Systems. IEAGHG.

Ingersoll Rand, 2019. Chemical Compatibility Guide. (accessed August 2019). www.arozona.com/en/aro-solution-center/tools/chemical-compatibility-guide.html.

International Energy Agency, I, 2017. Energy Technology Perspectives. 2017. .

IPEX, 2019. Chemical Resistance Guides. (accessed August 2019). http://www.ipexna.com/resources/technical-library/.

ISM, 2019. Elastomers Chemical Compatibility Chart. (accessed August 2019). http://www.industrialspec.com/images/files/elastomers-chemical-compatibility-chart-from-ism.pdf.

Jiménez, A., Thompson, G.L., Matthews, M.A., Davis, T.A., Crocker, K., Lyons, J.S., Trapotsis, A., 2007. Compatibility of medical-grade polymers with dense CO_2. J. Supercrit. Fluids 42, 366–372.

Johnsen, K., Helle, K., Røneid, S., Holt, H., 2011. DNV recommended practice: design and operation of CO_2 pipelines. Energy Procedia 4, 3032–3039.

Kazarian, S.G., 2000. Polymer processing with supercritical fluids. Polym. Sci. Ser. C 42, 78–101.

Kazarian, S.G., Vincent, M.F., Bright, F.V., Liotta, C.L., Eckert, C.A., 1996. Specific intermolecular interaction of Carbon Dioxide with polymers. J. Am. Chem. Soc. 118, 1729–1736.

Kendall, J.L., Canelas, D.A., Young, J.L., DeSimone, J.M., 1999. Polymerizations in supercritical carbon dioxide. Chem. Rev. 99, 543–564.

Khawaja, M., Sutton, A.P., Mostofi, A.A., 2017. Molecular simulation of gas solubility in nitrile butadiene rubber. J. Phys. Chem. B 121, 287–297.

Kim, S.W., Sohn, J.S., Kim, H.K., Ryu, Y., Cha, S.W., 2019. Effects of gas adsorption on the mechanical properties of amorphous polymer. Polymers 11, 817.

King, M.B., Mubarak, A., Kim, J.D., Bott, T.R., 1992. The mutual solubilities of water with supercritical and liquid carbon dioxides. J. Supercrit. Fluids 5, 296–302.

Kjärstad, J., Skagestad, R., Eldrup, N.H., Johnsson, F., 2016. Ship transport—a low cost and low risk CO_2 transport option in the Nordic countries. Int. J. Greenh. Gas Control. 54, 168–184.

Klimeck, J., Kleinrahm, R., Wagner, W., 2001. Measurements of the(p,ρ,T) relation of methane and carbon dioxide in the temperature range 240 K to 520 K at pressures up to 30 MPa using a new accurate single-sinker densimeter. J. Chem. Thermodyn. 33, 251–267.

Knoope, M.M.J., Ramírez, A., Faaij, A.P.C., 2013. A state-of-the-art review of techno-economic models predicting the costs of CO_2 pipeline transport. Int. J. Greenh. Gas Control. 16, 241–270.

Knoope, M.M.J., Ramírez, A., Faaij, A.P.C., 2015. Investing in CO_2 transport infrastructure under uncertainty: a comparison between ships and pipelines. Int. J. Greenh. Gas Control. 41, 174–193.

Kuijper, M., 2011. Public acceptance challenges for onshore CO_2 storage in Barendrecht. Energy Procedia 4, 6226–6233.

Lainé, E., Grandidier, J.C., Benoit, G., Omnès, B., Destaing, F., 2019. Effects of sorption and desorption of CO_2 on the thermomechanical experimental behavior of HNBR and FKM O-rings - Influence of nanofiller-reinforced rubber. Polym. Test. 75, 298–311.

Mane, S., Gao, Z.-Y., Li, Y.-X., Xue, D.-M., Liu, X.-Q., Sun, L.-B., 2017. Fabrication of microporous polymers for selective CO2 capture: the significant role of crosslinking and crosslinker length. J. Mater. Chem. A 5, 23310–23318.

Marco Rubber & Plastics, 2019. Rubber O-Ring Chemical Compatibility Chart, O-Ring Material Resistance Guide. (accessed August 2019). https://www.marcorubber.com/o-ring-chemical-compatibility-chart.htm.

Martynov, S.B., Daud, N.K., Mahgerefteh, H., Brown, S., Porter, R.T.J., 2016. Impact of stream impurities on compressor power requirements for CO_2 pipeline transportation. Int. J. Greenh. Gas Control. 54, 652–661.

Merkel, T.C., Toy, L.G., 2006. Comparison of hydrogen sulfide transport properties in fluorinated and nonfluorinated polymers. Macromolecules 39, 7591–7600.

Michaels, A.S., Bixler, H.J., 1961. Solubility of gases in polyethylene. J. Polym. Sci. 50, 393–412.

Morland, B.H., Dugstad, A., Svenningsen, G., 2017. Corrosion of carbon steel in dense phase CO_2 with water above and below the solubility limit. Energy Procedia 114, 6752–6765.

Munkejord, S.T., Jakobsen, J.P., Austegard, A., Mølnvik, M.J., 2010. Thermo- and fluid-dynamical modelling of two-phase multi-component carbon dioxide mixtures. Int. J. Greenh. Gas Control. 4, 589–596.

Neele, F., Koornneef, J., Jakobsen, J.P., Brunsvold, A., Eickhoff, C., 2017. Toolbox of effects of CO_2 impurities on CO_2 transport and storage systems. Energy Procedia 114, 6536–6542.

Noothout, P., Wiersma, F., Hurtado, O., Macdonald, D., Kemper, J., van Alphen, K., 2014. CO_2 Pipeline Infrastructure – Lessons Learnt. Energy Procedia 63, 2481–2492.

Nylacast, L.C., 2018. Chemical Resistance Table. (accessed 14 November 2018). https://www.nylacast.com/wp-content/uploads/2016/08/Nylacast-Chemical-Resistance-Table.pdf.

Paciorek, K.L., Mitchell, L.C., Lenk, C.T., 1960. Mechanism of amine crosslinking of fluoroelastomers. I. Solution studies. 45, 405–413.

Parker, M.E., Meyer, J.P., Meadows, S.R., 2009. Carbon dioxide enhanced oil recovery injection operations technologies (Poster presentation). Energy Procedia 1, 3141–3148.

Pasricha, A., Wing, G., Kumar, V., Tuttle, M., Seeler, K., 2005. Effect of CO_2 sorption and desorption on the creep response of polycarbonate. Polym. Eng. Sci. 45, 1639–1644.

Patchigolla, K., Oakey, J.E., 2013. Design overview of high pressure dense phase CO_2 pipeline transport in flow mode. Energy Procedia 37, 3123–3130.

Patchigolla, K., Oakey, J.E., Anthony, E.J., 2014. Understanding dense phase CO_2 corrosion problems. Energy Procedia 63, 2493–2499.

Paul, S., Shepherd, R., Woollin, P., 2012. Selection of Materials for High Pressure CO_2 Transport. Third International Forum on the Transportation of CO2 by Pipeline, Newcastle June 2012.

Plastics Pipe Institute, 2019. TR-19/2007 - Chemical Resistance of Thermoplastic Piping Materials. (accessed August 2019). https://plasticpipe.org/pdf/tr-19_thermoplastic_pipe_for_transport_of_chemical.pdf.

Puleo, A.C., Muruganandam, N., Paul, D.R., 1989. Gas sorption and transport in substituted polystyrenes. J. Polym. Sci. Part B: Polym. Phys. 27, 2385–2406.

Race, J.M., Downie, M.J., Graham, R.S., George, M., Poliakoff, M., Gibbins, J., Brennan, F.P., Maroto-Valer, M.M., Drage, T., Charles, E.A., Allwood, R., Oakey, J.E., Mahgerefteh, H., 2009. Materials for Next Generation CO_2 Transport Systems (MATTRAN). (accessed. https://gtr.ukri.org/projects?ref=EP%2FG061955%2F1.

Richardson, S.M., Saville, G., 1991. Blowdown of Pipelines, Offshore Europe. Society of Petroleum Engineers, Aberdeen, United Kingdom, pp. 9.

Roussanaly, S., Jakobsen, J.P., Hognes, E.H., Brunsvold, A.L., 2013. Benchmarking of CO_2 transport technologies: part I—onshore pipeline and shipping between two onshore areas. Int. J. Greenh. Gas Control. 19, 584–594.

Rubin, A., Wang, C., 2012. Qualification of flexible dynamic risers for supercritical CO_2. In: Offshore Technology Conference. Offshore Technology Conference. Houston, Texas, USA. pp. 10.

Rütters, H., Stadler, S., Bäßler, R., Bettge, D., Jeschke, S., Kather, A., Lempp, C., Lubenau, U., Ostertag-Henning, C., Schmitz, S., Schütz, S., Waldmann, S., 2016. Towards an optimization of the CO_2 stream composition—a whole-chain approach. Int. J. Greenh. Gas Control. 54, 682–701.

Sanders, E.S., 1988. Penetrant-induced plasticization and gas permeation in glassy

polymers. J. Memb. Sci. 37, 63–80.

Santos, S., 2012. CO$_2$ Transport Via Pipeline and Ship. CCOP-EPPM Workshop, Indonesia.

Sarrasin, F., Memari, P., Klopffer, M.H., Lachet, V., Taravel Condat, C., Rousseau, B., Espuche, E., 2015. Influence of high pressures on CH$_4$, CO$_2$ and H$_2$S solubility in polyethylene: experimental and molecular simulation approaches for pure gas and gas mixtures. Modelling of the sorption isotherms. J. Memb. Sci. 490, 380–388.

Sawan, S.P., Shieh, Y.-T., Su, J.-H., 1994. Evaluation of The-lnteractions Between Supercritical Carbon Dioxide and Polymeric Materials (Report LA-UR-94-2341). Los Alamos National Laboratory Report.

Schrittesser, B., Pinter, G., Schwarz, T., Kadar, Z., Nagy, T., 2016. Rapid Gas Decompression Performance of elastomers – a study of influencing testing parameters. Procedia Struct. Integr. 2, 1746–1754.

Schweitzer, P.A., 2006. Corrosion of Polymers and Elastomers. CRC Press.

Seevam, P.N., Race, J.M., Downie, M.J., Hopkins, P., 2008. Transporting the Next Generation of CO$_2$ for Carbon. Capture and Storage: The Impact of Impurities on Supercritical CO$_2$ Pipelines, pp. 39–51.

Shafiq, U., Shariff, A.M., Babar, M., Ali, A., 2018. A study on blowdown of pressurized vessel containing CO$_2$/N$_2$/H$_2$S at cryogenic conditions. IOP Conference Series: Materials Science and Engineering 458 012077.

Shieh, Y.-T., Su, J.-H., Manivannan, G., Lee, P.H.C., Sawan, S.P., Dale Spall, W., 1996a. Interaction of supercritical carbon dioxide with polymers. I. Crystalline polymers. J. Appl. Polym. Sci. 59, 695–705.

Shieh, Y.-T., Su, J.-H., Manivannan, G., Lee, P.H.C., Sawan, S.P., Dale Spall, W., 1996b. Interaction of supercritical carbon dioxide with polymers. II. Amorphous polymers. J. Appl. Polym. Sci. 59, 707–717.

Sim, S., Cole, I.S., Bocher, F., Corrigan, P., Gamage, R.P., Ukwattage, N., Birbilis, N., 2013. Investigating the effect of salt and acid impurities in supercritical CO$_2$ as relevant to the corrosion of carbon capture and storage pipelines. Int. J. Greenh. Gas Control. 17, 534–541.

Skaugen, G., Roussanaly, S., Jakobsen, J., Brunsvold, A., 2016. Techno-economic evaluation of the effects of impurities on conditioning and transport of CO$_2$ by pipeline. Int. J. Greenh. Gas Control. 54, 627–639.

Srisang, W., Supap, T., Idem, R., Tontiwachwuthikul, P., 2014. Study of physical and chemical resistance of elastomers in aqueous MEA and MEA + CO$_2$ solutions during the carbon dioxide absorption process. Energy Procedia 63, 1415–1423.

Størset, S., Tangen, G., Wolfgang, O., Sand, G., 2018. Industrial Opportunities and Employment Prospects in Large-scale CO$_2$ Management in Norway. Report nr. 2018:0594, ISBN 978-82-14-6865-8. SINTEF, Norway.

Takajo, T., Takahara, A., Kichikawa, T., 2008. Surface modification of engineering plastics through swelling in supercritical carbon dioxide. Polym. J. 40, 716.

Tebodin Netherlands, B.V., 2011. CO$_2$ Liquid Logistics Shipping Concept (LLSC) Overall Supply Chain Optimization.

Thermo Scientific, 2019. Nalgene Plastic Labware Chemical Resistance Reference Guide. (accessed August 2019). http://tools.thermofisher.com/content/sfs/posters/LCD-Chemical-Resistance-Guide-GALSPCHEMRESPOSTER-EN.pdf.

Tuminello, W.H., Dee, G.T., McHugh, M.A., 1995. Dissolving perfluoropolymers in

supercritical carbon dioxide. Macromolecules 28, 1506–1510.

Verma, S., Oakes, C.S., Chugunov, N., Ramakrishnan, T.S., 2011. Effect of contaminants on the thermodynamic properties of CO$_2$-rich fluids and ramifications in the design of surface and injection facilities for geologic CO$_2$ sequestration. Energy Procedia 4, 2340–2347.

von Schnitzler, J., Eggers, R., 1999. Mass transfer in polymers in a supercritical CO$_2$-atmosphere. J. Supercrit. Fluids 16, 81–92.

Wang, C., Rubin, A., Von Solms, N., 2013. Qualification of polymer materials for High pressure CO$_2$ flexible pipe structures, OTC Brasil. In: Offshore Technology Conference. Rio De Janeiro, Brazil. pp. 11.

Wang, J., Ryan, D., Anthony, E.J., Wildgust, N., Aiken, T., 2011. Effects of impurities on CO2 transport, injection and storage. Energy Procedia 4, 3071–3078.

Wang, J., Zhu, W., Zhang, H., Park, C.B., 2012. Continuous processing of low-density, microcellular poly(lactic acid) foams with controlled cell morphology and crystallinity. Chem. Eng. Sci. 75, 390–399.

Wang, W., Zhou, M., Yuan, D., 2017. Carbon dioxide capture in amorphous porous organic polymers. J. Mater. Chem. A 5, 1334–1347.

Wetenhall, B., Aghajani, H., Chalmers, H., Benson, S.D., Ferrari, M.C., Li, J., Race, J.M., Singh, P., Davison, J., 2014a. Impact of CO$_2$ impurity on CO$_2$ compression, liquefaction and transportation. Energy Procedia 63, 2764–2778.

Wetenhall, B., Race, J.M., Downie, M.J., 2014b. The effect of CO$_2$ purity on the development of pipeline networks for carbon capture and storage schemes. Int. J. Greenh. Gas Control. 30, 197–211.

Williams, L.L., Rubin, J.B., Edwards, H.W., 2004. Calculation of Hansen solubility parameter values for a range of pressure and temperature conditions, including the supercritical fluid region. Ind. Eng. Chem. Res. 43, 4967–4972.

Woodward, R.T., Stevens, L.A., Dawson, R., Vijayaraghavan, M., Hasell, T., Silverwood, I.P., Ewing, A.V., Ratvijitvech, T., Exley, J.D., Chong, S.Y., Blanc, F., Adams, D.J., Kazarian, S.G., Snape, C.E., Drage, T.C., Cooper, A.I., 2014. Swellable, water- and acid-tolerant polymer sponges for chemoselective carbon dioxide capture. J. Am. Chem. Soc. 136, 9028–9035.

Xiang, Y., Xu, M., Choi, Y.-S., 2017. State-of-the-art overview of pipeline steel corrosion in impure dense CO$_2$ for CCS transportation: mechanisms and models. Corros. Eng. Sci. Technol. 52, 485–509.

Xu, M., Zhang, Q., Wang, Z., Liu, J., Li, Z., 2018. Cross impact of CO$_2$ phase and impurities on the corrosion behavior for stainless steel and carbon steel in water-containing dense CO$_2$ environments. Int. J. Greenh. Gas Control. 71, 194–211.

Zero Emission Platform, 2011. The cost of CO$_2$ transport - post-demonstration CCS in the EU, carbon capture, CO$_2$ transport, economics. Use and storage (CCUS) 1–53.

Zhang, C., Bai, Y., Sun, Y., Gu, J., Xu, Y., 2010. Preparation of hydrophilic HDPE porous membranes via thermally induced phase separation by blending of amphiphilic PE-b-PEG copolymer. J. Memb. Sci. 365, 216–224.

Zhao, D., Tian, Q., Li, Z., Zhu, Q., 2016. A new stepwise and piecewise optimization approach for CO$_2$ pipeline. Int. J. Greenh. Gas Control. 49, 192–200.

Zhao, X., Watkins, R., Barton, S.W., 1995. Strategies for supercritical CO$_2$ fractionation of polydimethylsiloxane. J. Appl. Polym. Sci. 55, 773–778.